International Journal of Bridge Engineering (IJBE), Vol. 5, No. 3, (2017), pp. 69-122

BRIDGE ANALYTICAL FRAGILITY DEVELOPMENT METHODOLOGIES
A State of the Art Review

Benazir F. Ahmed[1] and Kaustubh Dasgupta[2]

[1,2] Indian Institute of Technology Guwahati, Dept. of Civil Engineering, India
e-mail: benazir@iitg.ernet.in, kd@iitg.ac.in

ABSTRACT: The seismic assessment of bridges has been on ever-increasing demand owing to the crippling consequences of earthquakes on the integrity of the transportation networks of which the bridges are the most sensitive elements. It has been widely accepted that a priori assessment of vulnerability of a bridge to seismic damage helps towards critical pre-earthquake safety decisions regarding replacement or setting up appropriate retrofit strategy for the bridge with an objective of minimizing life and socio-economic losses during future earthquakes. This paper reviews the past studies on vulnerability assessment of various existing bridge types and configurations through the generation of analytical fragility curves and summarizes the various steps involved in different methodologies. Generation of fragility function is one of the key components of seismic vulnerability assessment. Past studies reveal that realistic fragility estimates are obtained through detailed analysis of bridge-foundation-soil system, reliable definition and quantification of damage states and identification of an optimal earthquake intensity measure corresponding to the particular bridge structural configuration and site-specific earthquake hazard.

KEYWORDS: Capacity model; Damage state; Ground motion intensity measure; Probabilistic seismic demand model; Seismic fragility.

1 INTRODUCTION

Bridges are the vital components of any transportation network, damages to which can lead to disruption. The non-functionality of a bridge due to seismic damages may lead to severe consequences on supply of commodities and rescue operations in the earthquake affected areas. As structural system, bridges have very less redundancy and this leads to increased vulnerability during strong earthquake shaking. Recent earthquakes, particularly the 1989 Loma Prieta and 1994 Northridge earthquakes in California, and the 1995 Kobe earthquake in Japan, have caused collapse of or severe damage to a considerable number of major bridges that were at least nominally designed for seismic forces [1].

Cases of failures and damages to various bridge components like piers, piles, bearings, abutments, joints as well as deck pounding and unseating during past earthquakes emphasize the fact that bridges may be vulnerable to severe damage during strong earthquakes.

Investigation of past failures and damages in bridges during earthquakes revealed many design deficiencies, namely (a) inadequate ductile detailing in the flexural plastic hinge zones, (b) inadequate shear strength in columns, (c) insufficient shear reinforcement at cap beam-column junction, (d) inadequate development of the column longitudinal reinforcement into the footing, (e) inadequate seat widths at bearings and (f) non-ductile bearings. Also, the bridge design codal provisions and the seismic zonation maps of various countries have been revised over the years, thus making the existing bridges deficient in meeting the current seismic design requirements. Past earthquake damage reports have also revealed many additional vulnerability factors like bridge skew, curvature, spatial variability and directivity of ground motion, soil liquefaction potential, lateral spreading etc. During earthquake shaking, skew bridges often rotate in the horizontal plane, thus tending to drop off the supports at the acute corners. This behaviour is triggered by oblique contact and results in coupling of longitudinal and transverse response, binding in one of the obtuse corners and subsequently rotation in the direction of increasing skew angle [1]. Similarly, bridge curvature may also lead to higher force and deformation demands in bridge components during earthquake shaking and subsequently make them vulnerable [2]. Other factors like spatial variation of ground motion can significantly induce the pounding potential and deck unseating, particularly in case of long multi-span simply supported bridges [3]. Ductility demands for bridge columns could be underestimated if the bridge is analysed using identical support ground motions rather than differential support ground motions [4]. Also, the maximum seismic demand may vary when the horizontal components of ground motion travel from any orientation to a bridge site, other than the bridge orthogonal axes, resulting in a different scenario of bridge seismic damage than that when the same ground motion components are considered along the bridge axes [5]. Vertical components of ground motion can greatly influence the force demands in columns and piles [6]. Soil liquefaction as well as lateral spreading can result in increased fragility of bearings, piles, embankment soil as well as probability of unseating of deck [7].

Hence, it is of utmost importance to determine the physical state (extent of damage) of the bridge in the face of the expected hazard level (seismic force demand) in future. Seismic assessment deals with evaluating the inherent resisting capacity of the bridge and thereby determining the degree of its damage susceptibility to the seismic hazard it is likely to be exposed to. Based on the assessment of the performance levels of the bridges under future earthquakes, responsible decision can be made whether the bridge structure is suitable for use or repair, or whether the losses are acceptable or not [8].

Seismic assessment thus plays a crucial role in the disaster response planning, direct monetary loss estimation, loss of functionality evaluation of highway systems and retrofitting decisions [9].

Seismic vulnerability of existing bridges is primary attributed to the different uncertainties in the design and behavior of various bridge components as well as the uncertainties in the earthquake shaking. The importance of the possible damage of such infrastructure elements in the economic and social context led to the need for a better evaluation of the seismic risk they are exposed to through a more integrated probabilistic prospective, which includes uncertainties in both seismic hazard and structural response [10]. Therefore, current seismic performance assessment methods have focussed more on fragility curves which evaluate the probability of reaching or exceeding a predefined performance state (slight, moderate, extensive, collapse) at varying levels of earthquake intensity [11].

Research activity in the field of seismic assessment of existing bridges was initiated following the 1971 San Fernando earthquake. Detailed research on the seismic vulnerability aspects has been carried out from time to time in various regions worldwide for various general bridge typologies. A large number of research activities on vulnerability assessment have been carried out throughout the United States such as for the bridge inventories of the Central and Southeast United States [12-18] and specifically for bridges typical of various regions within the United States [4, 6, 7, 19-47]. Similarly bridges assessment activities have been carried out in Italy [3, 48, 49], Greece [50], Germany [51], Hungary [52, 53], New Zealand [54], Iran [55, 56], Turkey [5], Algeria [57], India [58, 59], Taiwan [60-62], Korea [63] and Japan [9, 64].

2 SEISMIC VULNERABILITY ASSESSMENT METHODOLOGY

Vulnerability studies are in general undertaken employing relationships that express the probability of damage as a function of a ground motion parameter, since neither the input motion nor the structural behaviour can be described deterministically [65]. With the development of performance based earthquake engineering, probabilistic assessment methods against possible seismic hazard are being used for highway bridges. Fragility curves, which are conditional probability statements that give the likelihood that a structure will meet or exceed a specified level of damage for a given ground motion intensity measure, have been widely used in probabilistic seismic risk assessment of highway bridges when the information is to be developed for a multitude of uncertain sources like seismic hazard, soil-structure interaction, structural characteristics and site conditions [66]. For seismic loading, the fragility simply looks at the probability that the seismic demand placed on the structure (D) is greater than the capacity of the structure (C) at some performance level of interest, conditioned on a chosen Intensity Measure (IM) of seismic loading.

This evaluation is accomplished by the convolution of the capacity models, commonly referred to as limit state models and the demand models to obtain the probability of exceedance of a limit state for a given IM. Demand models relate structural response measures termed as Engineering Demand Parameters (EDPs) to earthquake intensity measures. Damage models then attempt to relate the EDPs to different levels of damage (Damage Measures, DM). A fragility function can be described in the form of an equation as

$$\text{Fragility} = \text{P}[\text{LS}|\text{IM} = \text{y}] \quad (1)$$

where: LS is the limit state or damage level of the bridge or bridge component, IM is the ground motion intensity measure and *y* is the realization of the chosen IM. Thus, for earthquake shaking with a specific intensity measure, damage level may be predicted for any bridge with a defined fragility function (*Fig.* 1).

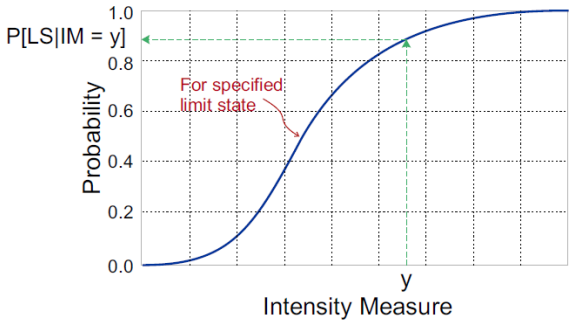

Figure 1. Typical fragility curve for an intensity measure [67]

For evaluating the fragility of a bridge, a system level approach is needed since the bridge system consists of multiple components (e.g., columns, decks, abutments and foundations) which introduce complex interacting behaviour due to the nonlinear behaviour of members, soil-structure interaction effects as well as geometric and structural constraints [68]. Hence, the choice of ground motion IMs, reliable EDPs as well as DMs, formulation of a nonlinear analysis model and incorporation of structural/ground motion variables sensitive to seismic responses form the key aspects of the methodology and these are summarized in the following sections.

2.1 Engineering demand parameters

The foremost requirement in the development of fragility curves involves the determination of bridge damage parameters. For estimating seismic damage, the capacity and demand computations required for bridge components are specified in terms of certain structural seismic response quantities expressed as EDPs with descriptor IMs. For the case of highway bridges, possible EDPs are grouped into 3 categories. Global EDPs describe overall bridge behaviour such

as maximum column displacement, drift ratio, abutment displacement, residual displacements etc. Intermediate EDPs describe the performance of bridge structural components such as maximum column curvature, column moment, shear force in the abutment etc. Finally, local EDPs describe material level responses (stress and strain) anywhere of interest in the bridge [11]. The selected EDPs should have direct and physical correlation with bridge level damages for obtaining reliable fragility curves. EDP selection is largely dependent on the structure; however, EDPs that describe the global behaviour of a structure typically result in demand models with lower uncertainty than localized demand measures. For bridges and buildings such efficient global EDPs are global drift ratios, or inter-storey drift ratios [69]. The most common EDPs monitored in most studies are column drift, curvature ductility, displacement ductility, pile-cap displacement, longitudinal and transverse deformation in the bearings, active, passive and transverse displacements in the abutment-wall and abutment-foundation.

2.2 Damage models and damage limit states

In numerical fragility analysis, the structural responses under earthquakes are depicted and monitored by various EDPs. A damage model is needed in which the observed damage and measured capacity of the structural components are correlated with the level of applied demand as a function of EDP [68]. Damage observations, i.e., the onset of certain damage states (DSs) are usually termed as Damage Measures (DMs). DSs are usually discrete and are marked by the associated limiting values (i.e. limit states LS) of the adopted DM. Traditionally, these limit states for bridge components have been defined by qualitative damage states such as slight, moderate, extensive and complete. Observable damage is introduced in the fragility formulation process by determining capacity and damage at different levels of structural response [11]. Damage models can be obtained from a large variety of sources. Sometimes termed capacity models, these can be described using a prescriptive (physics-based) approach, descriptive (judgment-based) approach or by incorporating both using Bayesian updating principles. The prescriptive approach is based on the mechanics of the problem where a functional level is associated with component damage such as concrete cracking, spalling in a column, buckling or rupture of the pier longitudinal reinforcement, transverse reinforcement fracture etc. In this mechanics-based approach which is usually the preferred method [70], limit states for the components are derived from the level of deformations or curvature demands or any other EDPs that correspond to physical damage of the components. The most common sources are experimental tests of structural components or systems or results of analytical methods such as pushover analysis. It is noted that uncertainties can also be introduced in the capacity model and contribute to the overall fragility. The median, S_c and the dispersion,

β_c values of the capacity limit states are obtained from experimental results [68]. The descriptive (judgemental) approach is based on the post disaster functionality level of the components and is usually in terms of repair cost and downtime [71] which would be assigned to the bridge by decision makers (bridge inspectors) for different levels of observed damage, thus making the approach a more subjective one [70]. Other options for limit-state definitions are evolving, such as the updating of these mechanics-based models with subjective data regarding functionality or closure decisions and repair cost implications. These approaches, however, require significant data for their characterization regarding historic failures, expert opinion, or field investigation [40].

The next step is to determine the damage state limits which are the ultimate values of the selected EDPs beyond which the bridge structure can no longer satisfy the specified performance level [5]. Bridge damage limit states have a direct influence on the reliability of the fragility curves, since these decide on meeting or exceeding of the bridge performance level for a given earthquake ground motion intensity parameter. Different codes and guidelines provide only qualitative damage limit state definitions for bridges. For example, five qualitative descriptions of damage states for highway bridge components are shown in Table 1. [72]. While assigning a particular damage level to a component, it is necessary to quantify those damage limit state definitions. Damage state limits in terms of the numerical values for the chosen EDPs (estimated using experimental results and analytical methods) are available in the past studies as discussed in the following section.

Table 1. Damage state definitions as per HAZUS [72]

Damage States	Definitions
None (ds_1)	No bridge damage
Slight/Minor (ds_2)	Minor cracking and spalling to the abutment, cracks in shear keys at abutment, minor spalling and cracks at hinges, minor spalling at the column (damage requires no more than cosmetic repair) or minor cracking to the deck
Moderate (ds_3)	Any column experiencing moderate (shear cracks) cracking and spalling (column structurally still sound), moderate movement of the abutment (< 2″), extensive cracking and spalling of shear keys, any connection having cracked shear keys or bent bolts, keeper bar failure without unseating, rocker bearing failure or moderate settlement of the approach.
Extensive (ds_4)	Any column degrading without collapse-shear failure (column structurally unsafe), significant residual movements at connections or major settlement approach, vertical offset of the abutment, differential settlement at connections, shear key failure at abutment.
Complete (ds_5)	Any column collapsing and connection losing all bearing support which may lead to imminent deck collapse, tilting of substructure due to foundation failure

2.2.1 Damage state and limits for piers

Commonly used EDP measures for columns are drift, displacement, curvature ductility, displacement ductility, curvature, flexural moment at the pier ends, concrete strain and steel strain and energy based damage indices. Pier drift was used as EDP for pier, defined as the ratio of relative displacement between the top and the base of the bridge piers to their height [6]. The adopted damage states as defined by slight, moderate, extensive and complete corresponded to reinforcement yielding, concrete cover spalling, two thirds of the displacement at the bar bucking and bar buckling respectively. Spalling and buckling limits were evaluated based on Barry and Eberhard equations [73] (Table 2.) as

$$\frac{\Delta_{sp}}{L}(\%) = 1.6\left(1 - \frac{P}{A_g f_c'}\right)\left(1 + \frac{L}{10D}\right) \quad (1)$$

$$\frac{\Delta_{bb}}{L}(\%) = 3.25\left(1 + K_{e_{bb}}\rho_{eff}\frac{d_b}{D}\right)\left(1 - \frac{P}{A_g f_c'}\right)\left(1 + \frac{L}{10D}\right) \quad (2)$$

where: Δ_{sp} is the column relative displacement at the onset of cover spalling,

Δ_{bb} is the column relative displacement at the onset of bar buckling,

$K_{e_{bb}}$ is 40 for rectangular-reinforced columns and 150 for circular columns,

ρ_s is volumetric transverse reinforcement ratio,

f_{ys} is yield stress of the transverse reinforcement,

d_b is diameter of the longitudinal reinforcing steel,

P is axial load

A_g is gross area of the cross section,

f_c' is the concrete compressive strength,

L is distance from the column base to the point of contraflexure,

D is the overall depth of the column section,

ρ_{eff} is $\frac{\rho_s f_{ys}}{f_c'}$

Five qualitative descriptions of performance levels of pier were attempted based on crack widths, crack angles, and regions of spalling (Table 3.) [74]. The performance levels were explicitly quantified with strain in concrete and steel as well as column drift as EDPs.

Four performance levels based on service as well as damage states were qualitatively identified for the wall piers used in their study (Table 4.) [42]. In order to quantify the damage levels, strain limits of concrete and steel were used as demand parameters and eventually generalized with wall drift as EDP from the results of pushover analysis as well as Incremental Dynamic Analysis (IDA) (Table 4.). Three damage states were adopted for piers based on material strains and the limits were identified in terms of displacement for the pier from the

results of pushover analysis for both longitudinal and transverse directions (Table 5.) [38]. Four damage states were identified for the bridge piers designed according to modern seismic codes and the corresponding limits were quantified in terms of pier displacement (Table 6.) [65] as EDP, monitoring the stress and deformations in the reinforcement, confined and unconfined concrete from pushover analysis of piers. Four damage states for piers were quantified in terms of column displacement due to the nonspecificity to a unique bridge pier [40]. Sectional analyses were performed for characteristic columns in Quebec to derive the limit states (Table 2.).

In another study, different damage states were based on elastic displacement limit, $\delta_{\xi,y}$ (conventional yield displacement) and ultimate displacement, $\delta_{\xi,u}$ (corresponding to strength drop of first pier, beyond which progressive failure of the bridge occurs, with successive pier failures) and limits were defined differently for high ductility bridges ($\mu_u \geq 3.0$) and for low-to-moderate ductility bridges ($\mu_u < 3.0$) (Table 2.) [50]. For existing bridges, with lack of confining reinforcement in piers (designed according to old regulations), two damage state limits were adopted for the bridge piers with peak drift ratio as EDP [8]. Eq.(2) and Eq.(3) were used to determine drift ratios on onset of cover spalling and bar buckling (Table 7.). The damage state definitions from [75] were adopted and limits were evaluated from pushover analysis in both longitudinal and transverse direction in terms of deck drift (Table 8) [76]. Drift as EDP for pier has also been used by [77] based on the result of real-scale tests on non-seismically and seismically designed piers, which were also transformed into corresponding rotational ductility (Table 9.).

Table 2. Correlation of damage states with pier drift [6] and pier displacement [40, 50]

Damage states	Drift ratio limits [6]	Displacement limits [40]	Threshold values of δ_ξ [50]	
			$\mu_u \geq 3.0$	$\mu_u \geq 3.0$
Slight	0.0076	5 mm	$> 0.7 \cdot \delta\xi, y$	$> 0.7 \cdot \delta\xi, y$
Moderate	Eq. 3	7 mm	$> 1.5 \cdot \delta\xi, y$	$> 1.5 \cdot \delta\xi, y$
Extensive	2/3Eq. 4	11 mm	$> 3.0 \cdot \delta\xi, y$	$> 3.0 \cdot \delta\xi, y$
Collapse	Eq. 4	30 mm	$> \delta\xi, u$	$> \delta\xi, u$

Table 3. Correlation of performance levels with concrete strain and steel strain and pier drift [74]

Performance level	Qualitative Description	Quantitative Description	Concrete strain	Steel Strain	Pier drift
I- Cracking	Onset of hairline cracks	Cracks barely visible	< 0.0032	< 0.005	<1
II- Yielding	Theoretical first yield of longitudinal reinforcement	Crack widths < 1mm	0.0032	0.005	1
III- Initiation of local mechanism	Initiation of inelastic deformation Onset of concrete spalling Development of diagonal cracks	Crack widths 1-2mm Length of spalled region >1/10 cross-section depth	0.01	0.019	3
IV- Full development of local mechanism	Wide crack widths /spalling over full local mechanism region	Crack widths > 2mm. Diagonal cracks extend over 2/3 cross-section depth. Length of spalled region >1/2 cross-section depth.	0.027	0.048	5
V- Strength degradation	Buckling of main reinforcement Rupture of transverse reinforcement Crushing of core concrete	Crack widths > 2mm in concrete core Measurable dilation > 5% of original member dimension	0.036	0.063	8.7

Table 4. Correlation of performance levels with column drift [42]

PL No	Service States	Damage States	Performance criteria	Column drift	
				PO	IDA
1	Immediate service	Minimal	Elastic behavior with minor damage Concrete compressive strain < 0.004 Steel strain < yield strain Fully serviceable, no service disruption	0.05	0.06
2	Limited service	Repairable	Inelastic behavior with moderate damage Concrete compressive strain < 0.006 Steel strain < 0.01 At least 50% lane remains operational	0.42	0.42
3	Service disruption	Extensive	Extensive visible damage Extensive spalling but no concrete crushing No fracture of hoops or buckling of longitudinal reinforcement Usable for restricted emergency traffic	0.98	1.02
4	Life safety	Near Collapse	Bridge will not collapse Life safety will be ensured	3.05	2.46

Table 5. Correlation of damage states with pier horizontal displacement [38]

Damage state	Damage description	Pier displacement	
		Longitudinal direction	Transverse direction
Serviceability	First yield of vertical reinforcing steel in tension	72 mm	36 mm
Damage control	Achievement of global maximum strength	124 mm	92 mm
Collapse prevention	Achievement of core concrete strain of 0.01 corresponded to 25% loss of core concrete stress, which resulted in a significant reduction in member strength	500 mm	260 mm

Table 6. Correlation of damage states with pier horizontal displacement [65]

Damage state	Damage state description	Limits
Undamaged	No damage, no yielding of vertical reinforcement bars	47 mm
Slightly damaged	Only minor structural damage and member flexural strength with limited ductility, but no concrete spalling in plastic hinges and that the crack widths remain sufficiently small	64 mm
Extensively damaged	Significant structural damage is expected The bridge will be out of service after the earthquake unless significant repair is undertaken However, repair and strengthening is feasible Rupture of transverse reinforcement or buckling of longitudinal should not occur and core concrete in the plastic hinge zones should not need replacement	103 mm
No collapse	Extensive damage is expected, but the bridge should not have collapsed Repair may be neither effective nor cost-effective The structure will have to be demolished after the earthquake Beyond this LS, global collapse endangering life is expected due to instability of the structure to sustain gravity loads Concrete strain corresponding to 50% of the concrete compressive strength and for steel strain of 9% are adopted for this limit state	142 mm

Table 7. Correlation of damage states with column drift [8]

Damage state	Damage state description	Drift
Minor	Minor damages in bridge columns with the onset of spalling of concrete cover (initiation of flexural damages) Functionality of bridge can be reduced and repairing cost are not negligible	.0155
Major	Onset of buckling of longitudinal bars Duration and costs of repairs can be significant and loss of bridge functionality can happened	.063

Table 8. Correlation of damage states with deck drift [76]

Damage State	Damage description	Deck drift	
		Longitudinal direction	Transverse direction
Fully operational	Negligible	<0.2	<0.5
Operational (LS-1)	Minor local yielding at some piers No observable fractures Minor buckling or observable permanent distortion of the bridge members	0.2–0.5	0.5–1.0
Life safety (LS-2)	Hinges form Local buckling of some elements Severe joint distortion Isolated connection failures A few elements may experience fracture	0.5–1.5	1.0–3.5
Near collapse	Extensive distortion for the structure components and pier panels Many fractures in connections	1.5–2.5	3.5–5.0
Complete collapse (LS-3)		>2.5	>5.0

Table 9. Correlation of damage states with drift [77] and rotational ductility [77, 81]

[77]					[81]	
Damage state	Description	Drift limits		Rotational ductility limits	Damage state	Rotational ductility limits
		Non-seismically designed	Seismically designed			
No damage	First yield	0.005	0.008	1.00	Minor	3.39
Slight damage	Cracking and spalling	0.007	0.01	2.01	Moderate	4.75
Moderate damage	Loss of anchorage	0.015	0.025	6.03	Major	8.43
Extensive damage	Incipient column collapse	0.025	0.05	11.07		
Complete damage	Column collapse	0.050	0.075	23.65		

To assess the overall seismic damage to a bridge, displacement ductility ratio, μ_d of a pier was adopted [25] and defined as,

$$\mu_d = \frac{\Delta}{\Delta_{cy1}} \quad (4)$$

where Δ is the displacement of a pier obtained from seismic response analysis of the bridge,

Δ_{cy1} is the displacement of a pier corresponding to the first yield of the vertical reinforcing bar.

The five seismic damage limit states [72] were quantified in terms of μ_{cy1} (the first yield displacement ductility ratio), μ_{cy} (the yield displacement ductility ratio corresponding to the yield curvature of the idealized moment curvature diagram of the pier section), μ_{c2} (the displacement ductility ratio with ε_c as 0.002 or 0.004 for pier with and without lap splice respectively) and μ_{cmax} (the maximum displacement ductility ratio, adopted according to [78] as μ_{c2}+3, assumed for poorly confined concrete pier) (Table 11.). In another study, pier damage state limits (both for seismic and non-seismic designed piers) were quantified in terms of displacement ductility (Table 10.) [61]. μ_f corresponds to ductility at occurrence of flexure to shear failure.

Rotational ductility as EDP was adopted in a number of studies [4, 79, 80] after transforming the column drift limits evaluated [77] (Table 9.). To define limits for the qualitative definitions as per [72], rotational ductility was utilized (Table 9.) [81]. The displacement ductility limits evaluated [25] were adopted and converted to the curvature ductility $\mu_\emptyset$ limits using the guidelines from [78] and used as EDP for the bridges (Table 10.) [67]. Curvature ductility was also adopted in another study [82]. Firstly the displacement ductility capacity corresponding to the damage states as per [72] was determined similar to [25] and then converted to curvature ductility according to [78] (Table 10.). For seismically and non-seismically designed piers, damage state limits were quantified in terms of curvature ductility [15] as per the recommendations of [25] and [73] (Equation (2) and (3)) (Table 12.). Curvature ductility was also adopted and limits were based on tests of non-seismically designed columns similar to those found in the bridges in their study (Table 12.) [12]. Curvature as EDP was also adopted to quantify the damage states for pier [34, 54] (Table 13.).

Table 10. Correlation of damage states with displacement ductility ratio [61]

Damage state	Damage limit criteria	
	Seismic design	Conventional design
Slight	$\mu = 2$	$\mu = 1$
Moderate	$\mu = 4$	$\mu = \min\,(1 + (\mu_f - 1)/2, 2)$
Extensive	$\mu = 6$	$\mu = \min\,(\mu_f, 3)$
Complete	$\mu = 9$	$\mu_f = 4.5$ or pier reaches its ultimate capacity

Table 11. Correlation of damage states with displacement ductility and curvature ductility ratios [25, 67, 82]

Damage state	Damage state description	Damage criteria	[25]	$\mu_{\emptyset}$	[67]	[82]
No	No yielding of Reinforcement bar	$\mu_{cy1} > \mu_d$	$\mu_d < 1$	$\mu_{\emptyset}$	< 1	< 1
Slight/Minor	First yield of vertical reinforcing bar	$\mu_{cy} > \mu_d > \mu_{cy1}$	$\mu_{cy1} = 1$	$\mu_{\emptyset y1}$	1	1
Moderate	Cracking of concrete	$\mu_{c2} > \mu_d > \mu_{cy}$	$\mu_{cy} = 1.2$	$\mu_{\emptyset y}$	1.58	2.39
Extensive	Spalling of concrete	$\mu_{cmax} > \mu_d > \mu_{c2}$	$\mu_{c2} = 1.76$	$\mu_{\emptyset 2}$	3.22	7.58
Complete	Longitudinal steel buckling	$\mu_d > \mu_{cmax}$	$\mu_{cmax} = 4.76$	$\mu_{\emptyset max}$	6.84	16.67

Table 12. Correlation of damage states with curvature ductility [12, 15] and Park-Ang damage index [9]

Damage states	Curvature ductility damage limits for pier			Park-Ang damage index
	[12]	[15]		[15]
		Non-seismically designed	Non-seismically designed	
Slight	$1.0 < \mu < 2.0$	1	1	0.14< DI <= 0.40
Moderate	$2.0 < \mu < 4.0$	1.58	1.58	0.40 < DI <= 0.60
Extensive	$4.0 < \mu < 7.0$	3.22	3.22	0.60 < DI < 1.00
Collapse	$7.0 < \mu$	4.18	4.18	1.0 <=DI

Table 13. Correlation of damage states with curvature [34, 54]

[34]		[54]	
Damage state	Limit	Damage state	Limit
First yielding of longitudinal column reinforcement	.0028/m	Cracking	0.00055/m
Beginning of column plastic hinge formation	.0035/m	Yielding	0.0036/m
Beginning of column strength degradation	.014/m	Spalling/buckling	0.0080/m
Ultimate compression strain at the column outer fibre	.035/m	Axial failure	0.0150/m

Four damage states for piers were quantified based on the flexural response, (i.e., the bending moment M of the pier) as EDP with and without lap splices respectively [25]. Damage description corresponding to each damage state and its limit state criteria are prescribed based on the moment capacity M_1 (column moment at the first yielding of longitudinal bar) and M_y (yield moment at the idealized moment curvature diagram of the pier sections) (Table 14.). The pier end rotation (θ) is compared with the plastic hinge rotations (θ_{p2} and θ_{p4}) with the concrete compressive strain, ε_c as 0.002 and 0.004 with and without lap splices respectively at the pier bottom.
Two damage states were defined based on repair requirement which were quantified using material strain limits (Table 15.) [76]. It was mentioned that the proposed strain limits for the serviceability limit states are widely accepted. On the other hand, damage control level strain limits were dependent on the detailing of transverse reinforcement. The given damage control strain limits are valid for well detailed systems and they would not be appropriate for assessment of existing columns with insufficient transverse reinforcement. Park-Ang damage index, $ID_{P\&A}$ was used as EDP for pier in the study [9], limits of which were used later in another study [56] (Table 12.).

Table 14. Seismic damage criteria for piers with and without splice in flexure [25]

Criteria	Description of Damage
$M_1 > M$	No reinforcement steel yielding, minor cracking in concrete
$M_y > M \geq M_1$	Tensional reinforcement yielding and extensive cracking in concrete
$M \geq M_y$, $\theta < \theta_{p2}$ (θ_{p4})	Hinging in column, but no failure of column
$M \geq M_y$, $\theta > \theta_{p2}$ (θ_{p4})	Flexural failure of column

Table 15. Correlation of damage states with material strains [83]

Damage state	Damage state limits	
	Concrete strain limit (compression)	Steel strain limit (tension)
Serviceability- repair is not needed after the earthquake	.004 (initiation of concrete crushing)	.015 (residual crackwidth >1mm)
Damage control- only repairable damage	.018 (concrete is still repairable)	0.060 (incipient buckling of reinforcement)

2.2.2 Damage states and limits for bearings

Existing bridges employ a variety of bridge bearings including various types of steel bearings like high type, low type fixed as well as expansion bearings; elastomeric bearings with a plain rubber pad or rubber pads reinforced with reinforced steel laminates in layers or with steel dowels. Depending on their material of construction as well as their mechanism of movability, each bearing behaves differently and hence their damage mechanisms also differ. For example, in case of high type bearings, the motion associated with the

expansion bearing is based on a rocking mechanism while it is characterized by sliding in the case of the low type bearing. The damage states of bearings are determined based on experimental observations as well as consideration of the resulting pounding and unseating.

For the bridges in a number of studies [7, 12, 15, 34, 67], damage state descriptions for high type fixed bearings were adopted as per [72]. Respective limits were quantified in terms of displacement, δ (in mm) as EDP based on experimental results [84] (Table 16.). Three damage states for low type fixed bearings were defined and the respective limits were identified in terms of displacement, δ (in mm) as EDP (Table 17.) [38], based on the experimental results [84]. In the absence of further experimental data, in the study [38], the behaviour of high fixed bearings in transverse and longitudinal directions and the behaviour of expansion rocker bearings in the transverse direction were assumed to be similar to the transverse direction tests of low-type fixed bearings as obtained from tests [84]. The expansion rocker bearings were designed so that they do not incur damage in the longitudinal direction unless bearings are unseated with excess displacement. Hence the bearing does not contribute to the first two damage states. Only collapse prevention limit was adopted and defined as when the bearing rolls over and taken equal to the seat width of the bearing plate, i.e., 230 mm [38]. Damage states for high type rocker bearings and low type sliding bearings were based on instability which may cause the superstructure to move a considerable distance and fall off the bridge seat in the worst case (Table 18.) [34].

Table 16. Correlation of damage states with bearing displacement [12]

Damage States	Description of damage	Damage limit criteria
No damage	Bearing within elastic range	$\delta < 1.0$
Slight damage	Appearance of minor cracks in the concrete pedestal	$1.0 < \delta < 6.0$
Moderate damage	Prying of the bearings and severe deformation in anchor bolts Initiation of strength degradation	$6.0 < \delta < 20$
Extensive damage	Bond failure of the high strength anchor bolts and rocking of the bearing on the bedding material followed by cracking and spalling of concrete cover of the reinforced concrete pedestal beneath the masonry plate Subsequent loosening of the nuts and slight raising and bending of the anchor bolts	$20 < \delta < 40$
Complete damage	Extensive concrete cover cracking or spalling of the reinforced concrete pedestal of high-type fixed bearings Back and forth rocking of the bearing due to complete bond failure and even its overturning after the fracture of the anchor bolts beyond a typical seat width	$40 < \delta$

Table 17. Correlation of damage states with bearing displacement [38]

Damage states	Damage definitions	Damage limit criteria	
		Mean	COV
Serviceability	Occurrence of slippage at interfaces between bearing plates and between bearings and structural elements	4	0.25
Damage control	Damages to pintle pins, holes and anchor bolts Attainment of the lateral shear capacity of the pintle pins restraining the bearing movement	7	0.5
Collapse prevention	Loss of lateral resistance of bearing	11	0.75

Table 18. Correlation of damage states with bearing displacement [34]

Damage state		Limits
High type rocker bearing	Overturning of the bearing about the edge of the bottom of the rocker by rolling off the rocker on the masonry plate with the deformation exceeding the half the width of the rocker, which may lead to unseating of bridge deck.	153 mm
low type sliding bearings	Translation of the sliding plate over the bronze plate being larger than half the width of the masonry plate	102 mm

Typically, either the bearing displacement or shear strain is used to describe the damage states for elastomeric bearings [68]. For plain elastomeric bearings, displacement limits were set as EDP for the four damage states adopted (Table 19.) [61], where N is the seat length of a girder at the support. Displacement as EDP was also used for the two damage states used for plain elastomeric pads in their study [54]. For elastomeric bearings with no fastener or connecting device between the elastomeric bearings and the superstructure and substructure components, three limit states based on displacement as EDP were developed (Table 20.) [5]. Damage states for the plain elastomeric bearings were quantified in terms of displacements based on the geometry of the bearing after attainment of shear capacity (Table 21.) [40]. For the bearings with elastomeric pads and dowel bars (fixed dowel and expansion dowels), damage states were based on fracture of the bearing and unseating of the girder as a function of the size of the bearings and the width of the supports (Table 22.) [12, 67, 42]. The limits were adopted in terms of displacement, δ mm. For such bearings, shear response, V may also be used as EDP in identifying damage limits [25] considering yield and ultimate shear capacity V_{by} and V_{bu} (Table 23).

Table 19. Correlation of damage states with bearing displacement [54, 61]

[54]		[61]	
Damage state	Damage limit criteria	Damage state	Damage limit criteria
Minor movement	0.05m	Slight	Yield displacement
Unseating	0.25 m	Moderate	10 cm
		Extensive	20 cm
		Complete	min (40cm, 2N/3)

Table 20. Correlation of damage states of elastomeric bearing with displacement [5]

Damage state	Damage state description	Limit
LS1-Serviceability	Friction resisting force holding the elastomeric bearing at its place gets exceeded by seismic force. Bearings will thereby be no longer stable and superstructure starts to make permanent displacements leading to minor problems at the bridge	40.5 mm
LS2-Damage control	Due to large horizontal displacement, Superstructure girders fall over the pedestal and rests on the cap beam directly. This could cause excessive damage on the asphalt disturbing the traffic flow and affecting the functionality of the bridge	425.0 mm

Table 21. Correlation of damage states of elastomeric bearing with bearing displacement [40]

Damage states	Damage definitions	Limits
Slight Damage	Loss of shear capacity.	30 mm
Moderate Damage	Displacement exceeds the height of the bearing	60 mm
Extensive Damage	Displacement exceeds 50% of the width or length of the bearing	150 mm
Complete Damage	Displacement exceeds the bearing full width or length, implying potential unseating	300 mm

Table 22. Correlation of damage states with bearing displacements [12, 67, 42]

Damage state	Damage description [67]	Limits δ mm	
		Fixed dowel	Expansion dowel
No Damage	No noticeable damage	$\delta < 8.0$	$\delta < 30$
Slight Damage	Noticeable damage yet would likely not cause much in the way of closure	$8 < \delta < 100$	$30 < \delta < 100$
Moderate Damage	Realignment of deck may be required and also implies possible dowel fracture	$100 < \delta < 150$	$100 < \delta < 150$
Extensive Damage	Dowel fracture is assured and would likely require some degree of repair (girder retention) in addition to deck realignment. Unrestricted sliding occurs thereafter	$150 < \delta < 255$	$150 < \delta < 255$
Complete Damage	Deck unseating	$255 < \delta$	$255 < \delta$

Table 23. Correlation of damage states with bearing displacements [25]

Damage state	Description of damage	Damage limit criteria
No damage	No damage to A307 Swedge bolts	$V < V_{by}$
Yielding	A307 Swedge bolts yielding	$V_{by} \leq V < V_{by}$
Failure	A307 Swedge bolts broken	$V \geq V_{bu}$

For lead-rubber bearings, damage state limits were identified based on shear strain, γ as EDP [28]. Similarly the same limit states were adopted for the modern isolation bearings having similar mechanical properties as the lead-rubber bearings [68]. Although modern isolation bearings can experience shear strains up to 400% before failure, the maximum shear strain was limited to be 250% corresponding to 0.25m maximum displacement on the basis that large shear strains will be the result of large lateral displacements which will be prevented by pounding at the abutment or preceded by girder unseating (Table 24.). The shear strain is utilized to capture the damage states in bearings since it can better characterize the bearing behavior due to the direct dependence of the shear modulus and damping of rubber on shear strain [85] as well as its ability to take into account the bearing size [68]. For the Reston Pendulum Sliding Bearing, the damage state limits were evaluated in terms of displacement (Table 24.) [82]. Bearing drift, θ was used as EDP for the four damage states adopted in the study [79] (Table 24.).

Table 24. Correlation of damage states with bearing shear strains [28, 68], displacement [82] and drift [79]

Damage states	Damage state limit		
	[28, 68]	[82]	[79]
Slight Damage	$\gamma > .100\%$	50 mm	$\theta > .007$
Moderate Damage	$\gamma > 150\%$	100 mm	$\theta > .015$
Extensive Damage	$\gamma > 200\%$	150 mm	$\theta > .025$
Complete Damage	$\gamma > 250\%$	200 mm	$\theta > .050$

2.2.3 Damage states and limits for abutments

Past earthquakes have shown that there are essentially two types of abutment damage that can occur during seismic loading. The first, stability damage, is mainly caused by foundation failure due to excessive ground deformation or loss of bearing capacity of the soil through tilting, sliding, settling and overturning of the abutment and can cause a serious disruption in the use of the bridge. The other type of damage is component damage/actual damage to the abutment itself, caused by excessive soil pressures with increased relative displacement between the abutment and the soil and is more easily repaired than the stability damage [86].

For abutment backwall, wing wall and foundation, displacement was used as EDP and the damage state limits were evaluated from the force-displacement relationship of the abutment-backfill system (Table 25.) [40]. The damage state limits in terms of displacement for the abutment were evaluated both in active and passive action [12, 67]. Pile and abutment soil stiffness contributing to the passive action and only pile stiffness contributing to the active action were based on the recommendations of Caltrans [87]. Thereby the limits are identified on the abutment force-displacement curves for both directions (Table

26.). In the study [50], damage state limits for abutment-backfill system were also based on system displacement as EDP (Table 27.). The first limit was based on longitudinal gap closure displacement, δ_{gap} after which abutment-backfill got engaged. The other limits were based on the yield displacement, $\delta_{y,ab}$ and ultimate displacement, $\delta_{u,ab}$ corresponding to yield and ultimate force respectively. Curvature as EDP was also adopted for abutment and damage state limits are quantified (Table 27.) [54]. Three damage states were defined for the seat-type abutments used in the study [38], based on [87], and the corresponding limits were evaluated in terms of abutment displacement (Table 28.).

Table 25. Correlation of damage states with displacement [40]

Damage states	Damage definitions	Damage limits for abutment	
		Wall	Foundation
Slight Damage	First yield.	7 mm	4 mm
Moderate Damage	50% of the ultimate displacement	15 mm	20 mm
Extensive Damage	Ultimate displacement	30 mm	40 mm
Complete Damage	Twice the ultimate displacement	60 mm	80 mm

Table 26. Correlation of damage states with displacement [12, 67]

Damage state	Damage state limits (δ, mm)	
	Passive action	Active action
Displacement below half of first yield	$\delta < 7.0$	$\delta < 4.0$
Displacement below first yield-soil yielding	$7.0 < \delta < 15$	$4.0 < \delta < 8.0$
Displacement below ultimate deformation	$15 < \delta < 37$	$8.0 < \delta < 25$
Pile in the plastic range	$37 < \delta < 146$	$25 < \delta < 50$
Displacement greater than twice the ultimate	$146 < \delta$	$50 < \delta$

Table 27. Correlation of damage states with displacement [50], curvature [54]

[50]		[54]	
Damage state	Damage limits	Damage state	Damage limits
Minor/Slight	δgap	Cracking	0.00055/m
Moderate	$> \delta y, ab + (1/3) \cdot (\delta u, ab - \delta y, ab)$	Yielding	0.0036/m
Major/Extensive	$> \delta y, ab + (2/3) \cdot (\delta u, ab - \delta y, ab)$	Spalling/buckling	0.0080/m
Failure/Collapse	$> \delta u, ab$	Axial failure	0.0150/m

Table 28. Correlation of damage state with displacement [38]

Damage state	Damage description	Damage limit
Serviceability	Soil pressure reaches its peak value of 369 kPa	25 mm
Damage control	Incipient damage to the abutments	61 mm
Collapse prevention	Severe traffic disruption due to backwall failure (attainment of wall shear strength due to a large impact from superstructure)	75 mm

2.2.4 Damage states and limits for piles

Ideally, the adopted EDP for pile damage should correlate perfectly with the occurrence of damage in the pile [88]. Pile cap displacement is a practically efficient EDP to assess pile foundation integrity and performance [7]. Many studies [6, 7, 29, 88, 89] quantified the pile damage in terms of pile cap displacement. The other competitive measure for pile damage representation is the curvature ductility of pile as it directly relates to the peak strains at the critical section of the pile and hence the extent of damage. However this EDP is a highly localized measure of demand whereas, the pile cap displacement gives a better account of the overall pile and foundation response [88]. Also the pile damage is easily computed in terms of pile cap displacement [89].

Pile cap displacement as EDP was adopted in a study [6] whereby pushover analysis of the pile (modelled with distributed plasticity throughout its length to capture the damage intended to occurs at various points along the pile's length) along with the surrounding soil (since the pile limit states are not only a function of design but also of the soil profile in which it is embedded) was carried out. Curvature capacity corresponding to first yield, second yield, two thirds of ultimate curvature, and ultimate curvature of the piles evaluated at varying levels of axial loads and related these to the pile cap displacements at the defined damage states. Based on the regression of the limit state capacities with respect to axial loads, Eqs.(5)-(8) were evaluated for pile cap displacement capacities at all the damage limits (Table 29.), which are given as,

$$\Delta_s = 2.15 \tag{5}$$

$$\Delta_m = 2.949e^{-7}P^2 - 4.669e^{-4}P + 3.14 \tag{6}$$

$$\Delta_e = 2.153e^{-7}P^2 - 2.962e^{-4}P + 8.11 \tag{7}$$

$$\Delta_c = 3.228e^{-7}P^2 - 4.4401e^{-4}P + 12.16 \tag{8}$$

where: Δ_s is the pile cap displacement capacity for slight damage,
Δ_m is the pile cap displacement capacity for moderate damage,
Δ_e is the pile cap displacement for extensive damage,
Δ_c is the pile cap displacement for complete damage,
P is the axial force of the pile (positive for compression) in kN

The pile cap displacement recommended [89] was also used as EDP in another study [90] to identify and quantify four damage states based on the fixed head concrete pile failure mechanism prescribed [91]. The limits were estimated based on the pushover analysis of pile in soil (Table 29.). Pile damage limit states were quantified also in terms of curvature along the pile length as EDP [54] (Table 30.). Qualitative descriptions for pile-soil system damages, considering soil failure, were prescribed based on the displacement limits to satisfy serviceability and ultimate failure criteria (Table 31.) [92].

Table 29. Correlation of damage states with displacement [6, 90]

Damage state	[6]		[90]	
	Damage description	Limits	Damage description	Limits
Slight	Attainment of first yielding curvature	Eq. 5	Formation of first plastic hinge at pile head	58.0 mm
Moderate	Attainment of second yielding curvature	Eq. 6	Formation of a second plastic hinge along the pile length	82.0 mm
Extensive	Attainment of 2/3 of ultimate curvature	Eq. 7	75% of the ultimate state	120 mm
Complete	Attainment of ultimate curvature	Eq. 8	Ultimate state associated with flexural failure, dictated by limiting curvature in the plastic hinge	160 mm

Table 30. Correlation of damage states with curvature [54]

Damage state	Limit
Cracking	0.0003/m
Yielding	0.0018/m
Failure	0.0060/m

Table 31. Correlation of damage states with displacement [92, 93]

Damage state	Damage description	Limits
Serviceability	The pile head deflection exceeds the tolerable head deflection. If pile displacement remains within a certain level and no notable residual displacement appears, it is expected that a steady horizontal soil resistance to piles is maintained and nothing is going to happen in service [93]	0.025 pile diameters [92] 1% diameter of pile [93]
Ultimate	The soil resistive stresses attain the limit (yield) value over a substantial portion of the pile length so that plastic flow occurs within the soil mass resulting in large lateral deflections, translation or rotation of the pile [92]	

2.3 Characterisation of Ground Motion

Fragility assessment generally evaluates the performance of a bridge/bridge components to a given earthquake ground motion hazard. The ground motion hazard is linked to the structural response through the term ‘Intensity Measure’ (IM) [94]. It is difficult to determine a single parameter that best characterises earthquake ground motion. Recorded time histories, even at the same site, show variations in details. Earthquake ground motion amplitude, frequency content, duration and the numbers of peaks (and even their sequence) in the time-history above a certain amplitude are some of the important characteristics that affect structural response and damage [65]. The input ground motion parameter, i.e., IM should be so selected that they correlate well with the structural response. Thus IMs should range from spectral quantities, across duration and energy related quantities, to frequency content characteristics.

The most commonly used IMs are (a) peak ground acceleration (PGA) [4,

12, 14, 23, 34, 38, 40, 61, 68, 70, 79, 80, 81, 95], (b) spectral acceleration at the geometric mean of the periods in longitudinal and transverse directions [14], (c) spectral acceleration at the fundamental period of the structure [4, 26, 76], (d) ratio of peak ground velocity to peak ground acceleration [26], (e) free-field lateral spreading ground displacement [29], (f) peak ground velocity [4] and (g) elastic spectral velocity [4]. Nevertheless many other IMs like peak ground displacement, elastic spectral displacement, inelastic spectral displacement, time duration of strong motion, Housner spectral intensity [4], Arias intensity, Root Mean Square Acceleration and perceived intensity (e.g. MMI, MSK, MCS, JMA etc) may be employed to describe the input motion severity. Each IM is ground motion specific and independent of the bridge model, except for period-based spectral quantities [96].

The fragility assessment largely depends on the characterization of the seismic demand for a structure and, for this reason, a proper or optimal IM is necessary [10] to better predict the EDPs chosen. The tracking and reducing uncertainties associated with PSDMs can be accomplished fruitfully only when the IMs upon which the demand model is conditioned is appropriate or optimal [97]. The choice of IM plays a crucial role both in running the fragility analysis and interpreting simulation results. It was suggested that in a logarithmic reference frame, the linear consistency of the results from probabilistic analysis can be an indicator of the applicability of the IM which is used to interpret the results [11]. Choosing an appropriate IM requires certain qualities to be fulfilled like sufficiency, practicality, efficiency, effectiveness and robustness.

The sufficiency condition is satisfied when the estimated EDP distributions depend only on the IM of the ground motion, not upon the properties of the records selected for analysis, i.e., the scenario by which it was reached (e.g., with no further dependence on variables such as the magnitude or distance of the causal earthquake) or else, it may result in a biased estimate of structural response. Similarly an IM is termed to be efficient if it can explain a large portion of a ground motion's effect on a structure, resulting in reduction in the remaining "variability" in EDP for that given IM. As such, fewer nonlinear dynamic analyses will be needed to characterize the relationship between structural response and the intensity measure; then, the possibility of biasing the structural response estimates is reduced [94]. An IM-EDP pair is "practical" if it has some direct correlation with known engineering quantities and makes engineering sense. Specifically, IMs derived from known ground motion parameters and EDPs from resulting nonlinear analysis are practical [96]. Practicality is measured by the regression parameter b in the PSDM. When this parameter approaches zero, the IM term contributes negligibly to the demand estimate. Therefore, a lower value of b implies a less practical IM [97]. With practicality being measured as correlation and efficiency being measured as dispersion, a term to measure their composite effect is beneficial. ζ, termed 'proficiency' was proposed to more effectively measure this composite

contribution [67] and serves as a primary factor in the selection process for an optimal IM [97].

"Effectiveness" of a demand model is determined by the ability to be evaluated in a closed form. For this to be accomplished, most of the studies assumed the EDPs to follow a log-normal distribution [96]. In that study, 23 different potential IMs were identified and compared for the development of PSDMs for multi-frame highway bridges. They found that spectral parameters at the fundamental period of the bridge (i.e., spectral acceleration and displacement) tended to be the most appropriate because of their tendency to reduce uncertainty in the demand model. For studies focussed on changing the design parameters, the use of S_d can be confusing, since the bridge period gets modified every time. Therefore, an IM is to be sought which is necessarily independent of the period, but still exhibits properties of an optimal PSDM. The spectral values can be considered as superior IM quantities as they not only incorporate measures of the motion frequency content, but are directly related to modal response of the given structure. Arias intensity does not include this structure-dependent information, but does, however, include the cumulative effect of energy input from the ground motion. PGA only has good correlation with response of structures with very small periods, as it is a spectral quantity for the zero second period structure. Depending on the fundamental period of the structure, a larger PGA does not necessarily indicate larger response. Most of the bridge structures of concern have first mode periods between 0.5 and 1.0 sec, thus explaining lack of correlation with PGA. PGD is a similar displacement based quantity. When considering pulse or fling type earthquakes, these two IMs may have more correlation with response [96]. Common period-independent IMs such as PGA do not produce efficient demand models for structures with longer periods. To eliminate the period-dependence (and hence structure-dependence) of the IM, peak ground velocity (PGV) was proposed as a more appropriate IM for bridges [69]. PGV and Spectrum Intensity, (SI) are better (based on reduced bias and uncertainty) IMs for such analyses of structures in liquefiable soils [54].

2.4 Uncertainties in capacity and demand

In a probabilistic framework, several uncertainty sources have to be considered. These uncertainties are typically classified as aleatoric and epistemic. Aleatoric uncertainty, also known as statistical uncertainty, is associated with inherent and inevitable randomness in the system or process and therefore can only be managed and not reduced. Epistemic uncertainty is due to a lack of knowledge, ignorance or course modeling, can generally be reduced with the acquisition of additional information and understanding [67]. In bridge engineering in particular, the most common source of aleatoric uncertainty is associated with the variability in the material properties of structural members (e.g., concrete, steel reinforcement, and bearing) and underlying soil properties. Similarly,

epistemic uncertainty is mainly related to the decisions made in finite element modelling. Ground motion uncertainty is to be addressed by carefully selecting suites of earthquake records that are compatible with the seismotectonic characteristics and the seismic hazard level at the site of interest [98]. Traditionally, randomness in seismic ground motions is considered to be aleatoric in nature, however when dealing with synthetic ground motions, the uncertainty built into these ground motions can not only be attributed to seismological mechanisms but also path and site characteristics. More knowledge pertaining to attenuation relationships and soil effects can reduce some of this uncertainty, thereby alluding to its epistemic nature [67].

Structural as well as geotechnical parameters and input motion characteristics (e.g., frequency contents, phase, and duration) have influence on structural damage which again affects the fragility curves [9]. Fragility curves for portfolios of structures therefore have the complexity of having to deal with the uncertainties [99] in geometric properties, structural and geotechnical material properties, component response parameters, seismic demand all of which are incorporated as random variables. The variation in these random variables is estimated based on the published literature, as well as engineering judgement [38]. Thereafter Empirical Cumulative Density Functions (CDF) are developed for each of these parameters [15].

The most common uncertain parameters used in most studies are compressive strength of concrete and the yield strength of reinforcing steel [12, 15, 34, 38, 40, 69, 70, 100], bridge mass [34, 40, 69, 70, 100], friction coefficient of bearings [15, 34, 37, 70, 100], bearing shear modulus [4, 32], dowel bar strength [15], gap at the dowels [15], expansion gap size [12, 34, 40, 70, 100], coefficient of thermal expansion [12], deck length [40], deck width [15, 40, [99], the ratio between the largest span length and total length of the bridge [40], column height [15, 40, 69, 99], column diameter [69], stiffness of the abutments and foundations [40, 15, 70], damping [40, 70], ratio of vertical reinforcement [69], number of spans [15], span length [15, 99], Rayleigh damping [15] and the angle of incidence of ground motions [15, 70, 99]. Similarly to account for variability in seismic demand, the uncertainties in seismic source, path attenuation, and local soil conditions, dynamic soil parameters like undrained shear strength, shear wave velocity, soil density, shear modulus are to be considered [37].

Due to a number of uncertain modeling parameters, many researchers did parametric studies to evaluate the sensitivity of the bridge's seismic response to variations in its structural and geotechnical parameters, to assess which modeling parameters significantly affect component responses. Method of Analysis of Variance (ANOVA) [40, 67] is generally performed to assess which modeling parameters significantly affect component responses. The study performed a hypothesis test of the significance of varying the modeling parameters over their range of potential realizations for each of the critical

bridge responses. A null hypothesis is tested which states that the coefficient of regression for the multiple linear regression model of the experiment is zero (or the effect of varying the parameter as insignificant).

Having identified the significant variables, the next step is to generate nominally identical but statistically different bridge samples with a range of randomly generated modeling parameters. It can be done using Latin

Hypercube Sampling technique (LHS). LHS has become popular in the recent past in probabilistic analysis, particularly for the random simulation of structural response variables, whose statistical distribution is known. [101]. LHS involves sampling N values from the prescribed distribution of each of k variables (x_1, x_2, ……, x_k). The cumulative distribution for each variable is divided into N equiprobable intervals with equal probability (N= the number of input motions at the specified seismic hazard level) and a value is selected randomly from each interval. The N values obtained for each variable are paired randomly with the other variables [40]. In the nonlinear time history simulations, these sets are then also matched randomly to the input ground motions (*Fig. 2*). LHS causes the entire range of each random variable to be represented in the set of variables used in the simulation. For a given number of random samples (of all random system properties), the variance in the response statistics obtained from LHS is smaller than that obtained from basic Monte Carlo simulation [102].

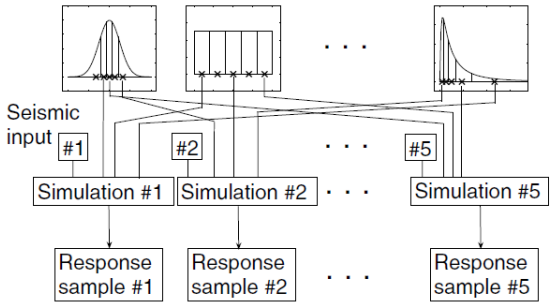

Figure 2. Latin hypercube sampling [102]

2.5 Fragility curve development

Describing the resulting structural performance as safe or unsafe is misleading when considering the uncertainty inherent in not only the seismic hazard, but also in structural capacity and function. Therefore, current seismic performance assessment methodologies are tending toward fragility curves as a means of describing the fragility of structures, such as highway bridges, under uncertain input. Fragility curves describe probabilities of exceedance of design or performance criteria at different levels of seismic input intensity. For each limit state, there is a unique CDF with ground motion intensity measure IM values on

the horizontal axis as an outcome of fragility analysis [96]. In the process of developing bridge fragilities, IMs are first coupled with EDPs to formulate Probabilistic Seismic Demand Models (PSDMs). Two damage models are then formulated. Component damage models utilize experimental data to predict response levels at which observable damage states are reached. System damage models utilize finite element reliability analysis to predict the loss of lateral and vertical load-carrying capacities [103].

Fragility curves can be derived using either empirical or analytical method. Empirical fragility curves are generated by statistical analysis of post-earthquake inspection of damage data from several recent earthquakes while the analytical fragility curves are the outputs of nonlinear dynamic analysis or quasi-static analysis when actual bridge damage and ground motion data are not available or inadequate. The fragility curves developed empirically seem to be more reliable since they are based on the more complete ground motion and actual bridge damage data [67]; however it has limitations. The foremost limitation is that the empirical fragility curves require a large amount of data for a particular damage state for a certain class of structures to get statistically significant results. In practice, this is only achievable through the combination of data from different earthquakes and locations [104] or through grouping classes together to get enough data for a given damage state and hence reduces the usefulness of the fragility curves [67]. The type of structure, structural performance (static and dynamic) and variation of input ground motion are usually not incorporated while constructing empirical fragility curves [9]. It is also found that the fragility curves (structural damages) are highly dependent on duration, amplitude and the spectral characteristics of the input ground motion and the empirical fragility curves cannot introduce various structural parameters and characteristics of input motion. Hence, analytical method is required to construct the fragility curves for a class of bridge structures, for which seismic behavior has not been documented for a large number of earthquakes.

2.5.1 Analytical fragility curve generation methodology

Because of the inherent deficiencies of the fragility curves generated empirically, most of the researchers have assessed seismic vulnerability through the fragility curves developed analytically. Analytical vulnerability curves adopt damage distributions simulated from the analyses of structural models under increasing earthquake loads as their statistical basis [104]. Fragility curve methodologies using analytical approaches have become widely adopted because of the ease and efficiency by which data can be generated, and hence can be readily applied to various bridge types and geographical regions with limited seismic bridge damage records. Different researchers used different analytical methods for simulating the bridge seismic response and generating the corresponding fragility curves.

In a past study, elastic spectral analysis was adopted to estimate capacity/demand (C/D) ratios for the bridge components [24], with the seismic capacity and the seismic demand determined from separate studies [73 and 105]. For an IM level, the bridge damage data assessed in terms of the C/D ratios of bridge components are statistically analysed and the results are represented using fragility curves.

Although an elastic analysis method gives a good indication of the elastic capacity of a structure and indicates where first yielding will occur, it cannot predict the failure mechanisms or account for redistribution of forces during progressive yielding. The evaluation using inelastic procedures provides better understanding as to how the structure will behave when subjected to major earthquakes, where it is assumed that the elastic capacity will be exceeded by providing an insight into the data on strength and ductility of the structure [106]. Hence, most of the researchers while generating fragility curves employ either one or both of the most common nonlinear analysis tools in the form of the nonlinear dynamic method employing ground motion time histories and capacity spectrum method employing pushover analysis. The fragility curve generation is summarized below from the perspective of nonlinear dynamic and static methodologies, most widely utilized for computing the seismic response of the bridges.

2.5.1.1 Nonlinear dynamic method

Fragility curve generation through nonlinear time history analysis has been adopted in many research work like [2-7, 9, 11-18, 23, 25-30, 34, 35, 37, 38, 40, 41, 52, 54, 58, 67, 70, 76, 81, 95, 98, 107-112] to estimate seismic demands on the bridge components. Inelastic time history analysis provides the most reliable solution to the prediction of forces and cumulative deformation (damage) demands in every element of the structural system as it accounts for the dynamic effects in the structure. The implementation of such a solution requires a set of ground motion records to account for the uncertainties and differences in severity, frequency characteristics and duration due to rupture characteristics and distances of the various faults causing the motions at the site [113].

The methodology involves the generation of PSDMs which establish a relationship between the peak demands on various components (columns, bearings, abutments, etc.) and a ground motion IM, i.e., to estimate the probability distribution of an EDP as a function of the IM [94] which is a major step in performance-based earthquake engineering assessments [114].

PSDM and Component Fragility Curve

The PSDMs are generated based on numerical simulations of 3D bridge model samples (incorporating random parameters) with nonlinear time history analyses (NTHA) as below:

a) A suite of N ground motions is assembled to represent the seismic hazard of

the region under consideration. The selected suite of ground motions applicable to the geographical area of interest should represent a broad range of values for the chosen intensity measure.

b) LHS technique as discussed in section 2.4 is used to generate statistically significant and nominally identical bridge models [7, 12, 34, 40].

c) The N adopted ground motions are then randomly paired with the analytical model of each of the N bridge sample models and the nonlinear time history analyses are performed on each bridge-ground motion pair to obtain the peak responses in each case. It is presumed that the demands placed on bridge components are dependent upon the properties of the components of the system due to sampling and allows for the propagation of the ground motion uncertainties [97]. There are two analysis approaches for generating PSDM which are discussed as follows:

   i) PSDA

   Probabilistic Seismic Demand Analysis (PSDA) uses a set of ground motions with associated *IM* values. The records are either left unmodified, or all records are scaled by a constant factor if the unmodified records are not strong enough to induce the structural response at the level of interest. The set of *IM* values and their associated *EDP* values resulting from nonlinear dynamic analysis are sometimes referred to as a "cloud," because they form an approximate ellipse when plotted [94].

   ii) IDA

   Incremental Dynamic Analysis (IDA) or the scaling approach uses ground motions all scaled to selective intensity levels corresponding to prescribed seismic hazard levels and analysis is performed at different hazard levels until the structure reaches certain predefined limit states. The resulting plot of EDP versus IM when all the records are scaled to a particular IM value looks like a "stripe". When the procedure is repeated over a range of IM values, multiple stripes of data can be obtained over a range of IMs. Several stripe analyses together are termed an "incremental dynamic analysis" (IDA) [115].

d) The peak responses of the components are plotted against the IM of the respective ground motions to develop the PSDMs. The choice of an estimation method for probability distributions of the EDP of interest as a function of ground motion intensity depends on whether distribution estimates are needed for a wide or narrow range of *IM* levels or for only a single level [94].

While using PSDA, PSDM uses the parametric approach where one assumes that the random variable *EDP* has some probability distribution (e.g., normal or lognormal) which is defined by only a few parameters [116]. Generally the choice of a distribution is made based on past experience, and statistical tests exist to identify when a dataset is not well represented by the specified

distribution (although with a small dataset it is difficult for such methods to confidently identify a lack of fit).

Using PSDA, most studies assumed the EDP data to have a lognormal distribution when conditioned on IM. Thus the conditional mean of EDP for a given IM is linear in log space, and the conditional dispersion of EDP for a given IM is constant; these often provide a reasonable estimate of the mean value of lnEDP over a small range, yielding the model (Eq.(9)). This power law model representation has been used widely, but is not necessarily the only possible model to express seismic demand as a function of an IM.

$$\overline{\mathrm{EDP}} = \ln a + b \ln \mathrm{IM} \quad + e \tag{9}$$

where: a and b are constant coefficients to be estimated from the regression analysis on the cloud of PSDA data,
e is a zero-mean random variable representing the remaining variability in $\ln EDP$ for a given IM.

After estimating the coefficients a and b from regression with this cloud (*Fig. 3*), the conditional mean of EDP for a given IM value, im can be computed using Eq.(9). If e is assumed to have a constant variance for all IM (a reasonable assumption over a small range of IM, but usually less appropriate for a wide range of IM), then the standard deviation of simulation data from the logarithmic correlation between median EDP and IM can be estimated as,

$$\beta_{\mathrm{EDP}\,|\,\mathrm{IM}} \cong \sqrt{\frac{\sum_{i=1}^{N}(\ln\,\mathrm{edp_i} - (a + b \ln \mathrm{im_i})^2}{N-2}} \tag{10}$$

where: $\mathrm{edp_i}$ is the EDP value of record i,
$\mathrm{im_i}$ is the IM values of record i,
N is the number of records.

Subsequently the EDPs are compared with the limit states (LS) corresponding to various damage states (DS). By further assuming a log-normal distribution of EDP at a given *IM*, the fragility functions (i.e., the conditional probability of reaching a certain damage state, d for a given IM) can be evaluated as in Eq. (11) and the probability values corresponding to each damage state for the range of IM values can be plotted versus IM to obtain the fragility curve for each component for each damage state (*Fig. 4*).

$$\mathrm{P[EDP} \geq \mathrm{d|IM]} = 1 - \Phi\left[\frac{\ln(\mathrm{edp}) - \ln(a\mathrm{IM}^b)}{\beta_{\mathrm{EDP}\,|\,\mathrm{IM}}}\right] = 1 - \int_0^{\mathrm{d}} \frac{1}{\sqrt{2\pi}\cdot\beta_{\mathrm{EDP}\,|\,\mathrm{IM}}\cdot\mathrm{edp}} \cdot \exp\left\{-\frac{[\ln(\mathrm{edp}) - \ln(a\mathrm{IM}^b)]^2}{2\left(\beta_{\mathrm{EDP}\,|\,\mathrm{IM}}\right)^2}\right\} \mathrm{d(edp)} \tag{11}$$

Eq. (11) also tends to simplify the mathematics required to manipulate it [67].

While using IDA, PSDM uses non-parametric approach which does not require assumptions about the distribution of the data [117]. These approaches have the advantage being robust when the data do not fit a specified parametric distribution, at the cost of reduced efficiency when the data do fit a specified parametric distribution [94].

The occurrence ratio of a specified damage state using IDA can be computed and directly used as the damage probability at the given IM level, i.e. the damage probability is calculated as the ratio of the number of damage cases n_i for the damage state i over the number of total simulation cases N [68] (Eq. (12).

$$P[EDP \geq d|IM] = \frac{n_i}{N} \ (i = 1 \ to \ n) \tag{12}$$

In most cases, IDA fragility curves can be fitted with either a normal cumulative distribution function (Eq.(13)) or a log-normal cumulative distribution function (Eq.(14)) as,

$$\mathrm{P[EDP \geq d|IM]} = \int_{-\alpha}^{\mathrm{IM}} \frac{1}{\sqrt{2\pi}\cdot\sigma_{\mathrm{IM}}\cdot \mathrm{d}} \cdot \exp\left[-\frac{(\mathrm{im}-\mu_{\mathrm{IM}})^2}{2\ {\sigma_{\mathrm{IM}}}^2}\right] \mathrm{d(im)} \tag{13}$$

$$\mathrm{P[EDP \geq d|IM]} = 1 - \int_{0}^{\mathrm{IM}} \frac{1}{\sqrt{2\pi}\cdot\beta_{\mathrm{IM}}\cdot \mathrm{im}} \cdot \exp\left\{-\frac{[\ln(\mathrm{im})-\lambda_{\mathrm{IM}}]^2}{2\ {\beta_{\mathrm{IM}}}^2}\right\} \mathrm{d(im)} \tag{14}$$

where: σ_{IM} and μ_{IM} are standard deviation and mean value of *IM* to reach the specified damage state based on the normal distribution,

β_{IM} and λ_{IM} are standard deviation and mean value of $\ln IM$ to reach the specified damage state based on the lognormal distribution.

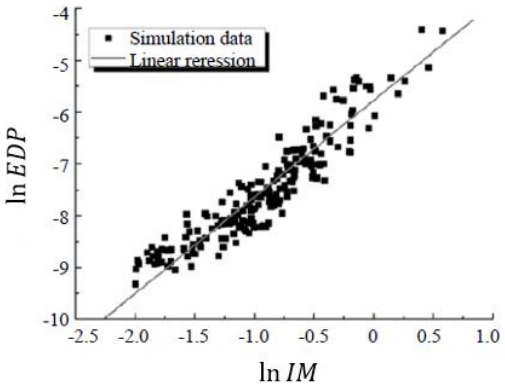

Figure 3. Data points of structural responses versus the corresponding IM and the linear regression [28]

Unlike PSDA, in IDA, the standard deviation is usually not constant over the considered range of IMs and also the mean value of $\ln EDP$ is not a linear function of $\ln \mathrm{IM}$. The advantage of using IDA over PSDA is that it is a direct

method if estimating the response at only a single IM level is of interest. However if the response estimates are needed at many IMs, IDA potentially requires more structural analyses than the cloud approach.

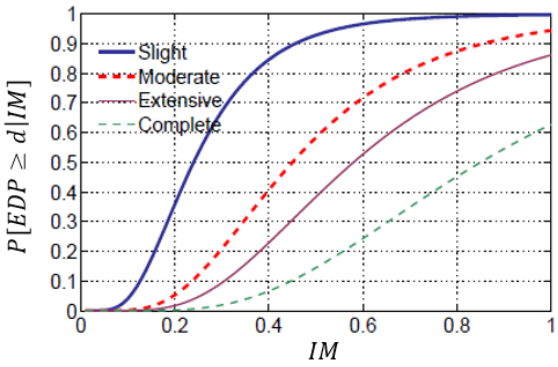

Figure 4. Fragility curves corresponding to slight, moderate, extensive and complete damage states [67]

Other than the regression analysis, Maximum Likelihood Method (MLM) is also used to estimate the parameters of a lognormal probability distribution describing the fragility curves [4, 66, 81]. If the fragility curve can be expressed in the form of two-parameter lognormal distribution function, the estimation of the two parameters (median and log-standard deviation) is performed with the aid of the MLM. Integrating the damage state information with that of the IM adopted, and making use of the maximum likelihood method involving the above equations, fragility curves can be constructed. This method can be used for any number of damage states. For better understanding, the analytical procedure was demonstrated for four states of damage where events E_1, E_2, E_3 and E_4 respectively, indicate the state of no, at least minor, at least moderate and major damage [4]. $P_{ik} = P(a_i; E_k)$ indicates the probability that a bridge *i* selected randomly from the sample will be in the damage state E_k when subjected to ground motion intensity expressed by IM = a_i. All fragility curves are represented by two-parameter log-normal distribution functions as,

$$F_j(a_i; c_i, \zeta_i) = \Phi\left[\frac{\ln\left(\frac{a_i}{c_i}\right)}{\zeta_i}\right] \tag{15}$$

where c_i and ζ_i are the median and log-standard deviation of the fragility curves for the damage state of "at least minor", "at least moderate" and "major" identified by j = 1, 2 and 3. From this definition of fragility curves, and under the assumption that the log-standard deviation is equal to and common to all the fragility curves, the equations obtained are

$$P_{i1} = P(a_i, E_1) = 1 - F_1(a_i; c_1, \zeta) \tag{16}$$

$$P_{i2} = P(a_i, E_2) = F_1(a_i;\ c_1, \zeta) - F_2(a_i;\ c_2, \zeta) \quad (17)$$

$$P_{i2} = P(a_i, E_2) = F_1(a_i;\ c_1, \zeta) - F_2(a_i;\ c_2, \zeta) \quad (18)$$

$$P_{i3} = P(a_i, E_3) = F_2(a_i;\ c_2, \zeta) - F_2(a_i;\ c_3, \zeta) \quad (19)$$

The likelihood function can then be introduced as

$$L(c_1, c_2, c_3, \zeta) = \prod_{i=1}^{n} \prod_{k=1}^{4} P_k(a_i\,; E_k)^{x_{ik}}, \quad (20)$$

where: x_{ik} is 1 if the damage state E_k occurs in the i^{th} sample bridge subjected to $a = a_i$, and is 0 otherwise.

Then the maximum likelihood estimates c_{0j} for c_j and ζ_0 for ζ are obtained by solving Eq.(21) as,

$$\frac{\partial \ln L(c_1,c_2,c_3,\zeta)}{\partial c_j} = \frac{\partial \ln L(c_1,c_2,c_3,\zeta)}{\partial \zeta} = 0 \qquad (j = 1,2,3) \quad (21)$$

by implementing a straightforward optimization algorithm.

System Fragility Curve Generation

Although the generated curves give an indication of the most vulnerable components in the bridge, the general assessment of seismic vulnerability for the overall bridge must be made by combining the effects of the various bridge components. In fact, it is often the case that the system vulnerability is strongly affected by the coupling between simultaneously developing damage modes in different components involving both the structure and its foundation [98]. It is observed that different components control the fragility of bridges for different levels of demand and different damage states. Therefore, it is necessary to combine the fragility curves for the components into a fragility curve for the entire bridge [40]. Ignoring the contributions of the major bridge components can lead to a misrepresentation of the overall fragility of the bridge [70]. The study found the bridge as a system to be more fragile than any one of the individual components. It was observed that assuming only the columns to represent the entire bridge system vulnerability can result in errors as large as 50% at higher damage states. Hence the logical step that succeeds the determination of component fragilities is to integrate these to enable the macroscopic view of the bridge as a system [15]. Several researchers [13, 67, 68] have proposed techniques to develop fragility curves for the bridge as a system.

The most commonly used technique in assessing bridge-system performance under seismic loading is a series system approximation adopted for bridge level failure analysis. In this method, bridge damage state is assumed to have achieved if 'any' component X 'or' component Y exhibits the associated level of damage. The probability that the bridge is at or beyond a particular limit state $Fail_{system}$ is the union of the probabilities of each of the n components exceeding the same limit state $Fail_{system-i}$ as,

$$P[Fail_{system}] = \cup_{i=1}^{n} P[Fail_{system-i}] \quad (22)$$

This system-level abstraction implies that, if at least one bridge component achieves a particular damage state, the overall bridge system is deemed to achieve that level of damage [40].

The bridge system can be assumed be a series as well as parallel combination of the individual components [68]. If a bridge is assumed to operate like a serial system with each component performing an indispensable role independently, then any component damage will result in system damage at the same level. Hence the global damage state is dictated by the largest damage state at component level, i.e.,

$$DS_{system} = \max(DS_{component1}, DS_{component2}, \ldots\ldots, DS_{componentN}) \quad (23)$$

The lower and upper bounds of the system fragility for a serial system are expressed as,

$$\max_{i=1}[P(F_i)] \leq P(F_{sys}) \leq 1 - \prod_{i=1}^{N}[1 - P(F_i)] \quad (24)$$

where: $P(F_i)$ is the probability of failure of component i
$P(F_{sys})$ is the probability of the system.

The lower bound corresponds to completely correlated components while the upper bound assumes no correlation among components. The real system fragility of bridge is located within these two bounds and the exact position depends on the correlation of the component responses.

On the other hand if a bridge is assumed as a parallel system, then it will reach a specific damage state when all components have reached that damage state. Therefore, the system damage state is dictated by the smallest damage state at component level, i.e.,

$$DS_{system} = \min(DS_{component1}, DS_{component2}, \ldots\ldots, DS_{componentN}) \quad (25)$$

The failure probability of a parallel system is computed as the intersection of component probability and its lower and upper bounds are given as,

$$\prod_{i=1}^{N} P(F_i) \leq P(F_{sys}) \leq \min P(F_i)] \quad (26)$$

The lower bound corresponds to independent components while the upper bound results from completely correlated components. These bounds are often very wide, which imply the significance of correlation between components. In reality, a bridge is neither a parallel nor a serial system and the responses of components are often correlated with each other to some extent. The first-order bounds shown in Eqs. (24) and (26), assuming either the total correlation or complete independence between components, are not able to provide an accurate estimation of the failure probability of the bridge system. The global damage state is hence located in between the limits set by Eqs. (23) and (25).

First order bounds were considered for series systems as an alternative to the more computationally demanding Monte-Carlo simulation to get the system

fragility curve [12]. The study found the lower bound representing the probability of failure for a system with fully stochastically dependent components to provide un-conservative estimate for the fragilities of the considered bridges. Similarly the upper bound assumes that the components are all statistically independent and was found to provide a conservative estimate on the overall bridge fragility. As the difference between the upper and lower bound decreases, the upper bound estimate of the system fragility becomes more appropriate. To account for seismic risk from multiple failure modes, second-order reliability was adopted where some correlation was evaluated and was found to yield narrower bounds than the commonly used first-order reliability method, thereby a single estimate for the second order fragility could be approximately obtained [34].

In another study, the estimate of the system or bridge level fragility is facilitated through the development of a Joint Probabilistic Seismic Demand Model (JPSDM) for including the effects of multiple bridge components [67]. This approach is in recognition that there is some level of correlation between the demands placed on the various bridge components during a given earthquake. Accounting for the correlation is important for fragility analysis when a vector of EDPs is utilized. Thus, the seismic demand on the system is simply the joint demand on the components. If $\underline{X} = (X_1, X_2, \ldots, X_n)$ represents the vector of demands, X_i, placed on the n components of the system, then the vector, $\underline{Y} = \ln(\underline{X})$ represents the vector of component demands in the transformed lognormal space. Since the marginal component demands, X_i, are lognormally distributed, the transformed demands, Y_i, are normally distributed in the transformed space. The JPSDM is formulated in this space by assembling the vector of means, $\mu_{\underline{Y}}$ and the covariance matrix, $\sigma_{\underline{Y}}$. It must be noted that the covariance matrix, $\sigma_{\underline{Y}}$, considers the correlation coefficients between $\ln(X_i)$ and not X_i. The correlation coefficients between the component demands are obtained by using the results of the NLTHA and the resulting covariance matrix is then assembled. A Monte Carlo simulation is then used to compare realizations of the demand (using the JPSDM defined by a conditional joint normal distribution in the transformed space) and statistically independent component capacities to calculate the probability of system failure. Samples are drawn from both the demand and capacity models and the probability of demand exceeding the capacity is evaluated for a particular IM value. The procedure is repeated for increasing values of the IM. Regression analysis is used to estimate the lognormal parameters, median IM value and and an associated dispersion value ζ, which characterizes the bridge system fragility [118] using the equation,

$$\mathrm{P}[\text{Damage State i or greater}|\mathrm{IM}] = \Phi\left[\frac{\ln(\mathrm{IM}) - \ln(\mathrm{med_i})}{\zeta_i}\right] \qquad (27)$$

where: $\mathrm{med_i}$ and ζ_i are the parameters belonging to the i_{th} damage state.

By developing the JPSDM, the system fragility can be directly estimated rather than using system bounds as has been done in previous studies [12]. The proposed fragility curve methodology thus eliminates the need to rely on system fragility bounds and their associated restriction to serial systems. It should be noted that the specifics on the application of this methodology will vary depending on the type of bridge being considered. For example, the number and type of bridge components to be considered may vary from one bridge type to another. Also, the capacity models used for one type of bridge may not be appropriate for another type [70].

However, the component fragilities should be combined in such a way that they have similar consequences at the system level in terms of functionality and repair consequences [67, 118]. The major challenge lies in being able to group components that have similar consequences at the system level in terms of functionality and repair consequences. A common question that could arise is: "Do the complete collapse of columns have the same effect on bridge functionality as the complete damage to a shear key or tearing of an elastomeric bearing pad?"[67]. In order to be able to address the aforementioned concerns, two classes of components viz., primary and secondary were proposed [144].

Primary components are defined as those that affect the vertical stability and load carrying capacity of the bridge. Extensive or complete damage to these components might lead to closure of the bridge. Column damage and deck unseating belong to this category. Secondary components may be defined as the ones that do not affect the vertical stability of the bridge. Failure of these components will not force closure of the bridge but might lead to restrictions on the travel speed and traffic conditions on the bridge. Shear key, bearing, and abutment are defined as secondary components.

The component-level damages, DC1-DC4 assigned to each of the system damage states, DS1-DS4 are presented in Table 32. where DC 1–4 do not correspond directly to the sequence of system level damage state. Instead, primary components contribute to all the system level damage states, while secondary components contribute to the first three system level damage states. The system fragility curves were derived considering the correlations between components as shown in Eq.(28) in which the probability of exceeding a system level j^{th} damage state, $P[DS_j|IM]$ is typically computed as the probability of the union of events $E_j[DC_j|IM]$ in which each of the i^{th} bridge components reaches or exceeds the j^{th} damage state.

Table 32. Assignment of component-level damage with system damage state [30]

Limit state	Component-level limit state		System-level limit state
	Primary component	Secondary component	
Slight	DC1	DC2	DS1
Moderate	DC2	DC3	DS2
Extensive	DC3	DC4	DS3
Complete	DC4	N/A	DS4

$$P[DS_j|IM] = \begin{cases} P\left[\cup_{i=1}^{N} E_{primary\_}i(DC_j|IM)\right] \text{ for } j = 4 \\ P\left[\cup_{i=1}^{N} E_{primary\_}i(DC_j|IM)\right] \\ +P\left[\cup_{m=1}^{M} E_{secondary\_}m(DC_{j+1}|IM)\right] \text{ for } j \leq 3 \end{cases} \quad (28)$$

where: N is the total number of primary components,
M is the total number of secondary components,
j is 1, 2, 3, 4 corresponding to the slight, moderate, extensive, and complete damage states, respectively.

A new system of bridge-level performance objectives has been proposed based on loss of bridge performance in terms of traffic load carrying capacity, loss of lateral and vertical load capacity (Table 33.) [11].

Table 33. Proposed performance levels using bridge-level damage variables [11]

Objective name	Traffic capacity remaining (volume)	Loss of lateral load carrying capacity	Loss of vertical load carrying capacity
Immediate access	100%	< 2%	< 5%
Weight restriction	75%	< 2%	< 10%
1 lane open only	50%	< 5%	< 25%
Emergency access only	25%	< 20%	< 50%
Closed	0%	> 20%	> 50%

Previous studies suggest that system fragility can be derived based on functionality or repair cost after an earthquake [11], or can be generated based on component level fragility functions [67]. In another study, the bridge system composite damage states, based on component damage states D_Ss, are devised as shown in Eq.(29) and the proportion ratio for columns and for bearings was determined synthetically [68].

$$D_S^{System} = \begin{cases} \text{int}(0.75D_S^{pier} + 0.25D_S^{bearing}) & D_S^{pier}, D_S^{bearing} < 4 \\ 4 & D_S^{pier} \text{ or } D_S^{bearing} = 4 \end{cases} \quad (29)$$

where: the numbers are 1, 2, 3, 4 refer to the damage states in increasing order

Taking into account the relative importance for load-carrying capacity during an earthquake and the repair cost after an earthquake, weighting ratios of 0.75 and

0.25 are assigned to pier columns and isolation devices respectively. This ratio reflects the fact that columns are more critical than isolation devices and will cost more to be repaired hence should carry more weight. However, since either excessive bearing displacement or column collapse damage (D_S=4) can result in the collapse of a single span or the entire bridge, a serial mechanism is therefore adopted for the collapse damage. For the fourth damage state, they applied the governing damage between the piers and isolators.

2.5.1.2 Capacity spectrum method

Nonlinear time history analysis for fragility curve development requires a lot of computational effort since a large number of simulations are required to derive the fragility functions. As an alternative, many researchers preferred and adopted a simpler and practice-oriented nonlinear static analysis procedure in the form of the Capacity Spectrum Method (CSM) for fragility curve generation. CSM was developed in 1970's for seismic vulnerability of buildings and used as a procedure to find a correlation between earthquake ground motion and building performance [119]. This method has been extended for fragility analysis of bridges by many researchers [22, 39, 44, 48, 50, 51, 55, 60, 120, 121]. CSM basically identifies the structural performance by superimposing the seismic demand spectrum onto the capacity spectrum of the structure. The key elements of CSM are discussed in this paper.

Capacity Spectrum

Capacity spectrum represents the capacity curve of the structure, transformed in spectral Acceleration-Displacement Response Spectrum (ADRS) format. The capacity curve is the equivalent SDOF representation of the pushover curve of the MDOF structure. The pushover curve, which is usually a plot of the total base shear, V_b at all the supports of the structure versus the displacement, u_N at the control node of the MDOF structure (*Fig. 5(a)*) is derived from the nonlinear static analysis in which the MDOF structure is subjected to monotonically increasing lateral forces/displacements at the nodes with an invariant distribution until the structure reaches a predetermined target displacement or collapse. The equivalent SDOF capacity curve is modeled using participation factor, Γ for the MDOF structure's vibrating mode and the modal mass representing the mass of the equivalent SDOF system corresponding to the masses, m_i of the MDOF model. Presuming that the loading shape vector (normalized), ϕ_i is known, Γ and m^* are calculated as,

$$\Gamma = \frac{m^*}{\sum m_i \phi_i^2}, \quad m^* = \sum m_i \phi_i \tag{30}$$

MDOF pushover curve force-displacement coordinates are divided by Γ to obtain the SDOF capacity curve. The ordinates are further reduced by m^* to obtain the capacity spectrum (*Fig. 5(b)*).

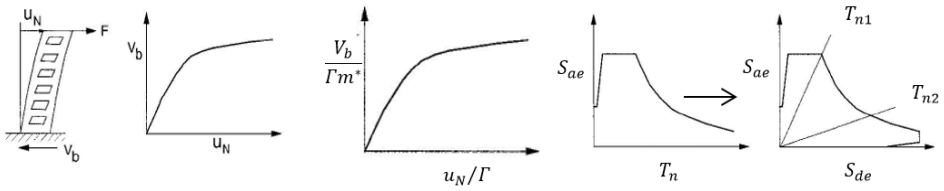

Figure 5. (a) Pushover curve, (b) capacity spectrum and (c) conversion of elastic response spectrum from standard format to ADRS format) [122].

Pushover analysis employed while generating the capacity spectrum has become the preferred analysis procedure due to its conceptual and computational simplicity, ease of use and capability of tracing the sequence of yielding and failure on member and structural level as well. It, however, requires as a matter of necessity a realistic pushover curve for the structure that is representative of its true dynamic behaviour under a seismic event. Although the conventional assumptions lead to rather good predictions of the maximum seismic response of the MDOF structures dominated by a single mode, it is inappropriate for structures with higher mode effects leading to inaccurate estimation of target displacement. Also the distribution of lateral inertia forces varies continuously during earthquake response; the invariant load pattern fails to keep track of the structure's dynamic characteristics change after the formation of the first local plastic mechanism. This method does not account for damage accumulation and resulting modification of the modal parameters, which might considerably affect the response characteristics of a given structure. Hence the accuracy and the reliability of pushover analysis in predicting global and local seismic demands for all structures have been a subject of discussion and improved pushover procedures have been proposed to overcome the certain limitations of traditional pushover procedures.

In order to improve the accuracy in the estimation of seismic response of structures with higher mode effects, a Modal Pushover Analysis (MPA) procedure was developed focussing on buildings [123]. Pushover analyses were carried out separately with the forcing vectors representing each of the significant modes and the contributions from individual modes are combined using a statistical combination rule to calculate the peak response quantities. The multi-modal procedure constitutes a significant improvement over the conventional pushover analysis, since it explicitly considers the response of more than one vibration mode and the influence of the expected ground motion, thus yielding results that are closer to rigorous inelastic time-history analysis. MPA has been used in studies for (a) multispan curved bridge [107, 124] and (b) irregular old bridge [125]. However it still retained the conceptual simplicity of procedures with invariant force distribution.

In order to overcome the limitations of the conventional methods, many studies adopted adaptive pushover analysis in which at each analysis step, it has the ability to adapt the load to be applied to the structure thus following more closely the time-variant distributions of inertia forces leading to conceptually more correct results. The dynamic properties of the structure are determined by the means of eigenvalue analyses that consider the instantaneous nonlinear structural stiffness and mass matrix. It accounts for both higher mode contributions as well as alteration of the local resistance and modal characteristics of the structure, as induced by the progressive accumulation of damage. Site- or record-specific spectral shapes can also be explicitly considered in the scaling of forces, so as to account for the dynamic amplification that expected ground motion might have on the different vibration modes of the structure [126].

The Force-based Adaptive Pushover (FAP) procedures (with force profile as loading), despite its apparent conceptual superiority, provides a relatively minor advantage over its traditional non-adaptive counterpart, particularly in what concerns the estimation of deformation patterns of buildings, which are poorly predicted by both types of analysis [127]. Application of displacements, rather than forces, in an adaptive fashion, with the possibility of updating the displacement loading pattern according to the structural properties of the model at each step of the analysis, can be a conceptually appealing deformation-based nonlinear static analysis tool [128]. It was shown that, in comparison to force-based alternatives, Displacement-based Adaptive Pushover (DAP) manages to provide greatly improved predictions, throughout the entire deformation range, of the dynamic response characteristics for different types of structures.

In a parametric study, it was observed that the conventional force-based procedure with first mode proportional load pattern performed well for regular bridges and underestimating otherwise [126]. DAP procedure features the best overall behaviour, despite the slight under prediction of the deformed shape values, with the lowest values of scatter. Recently, DAP was extended for a preliminary verification of the assessment of a series of concrete bridge configurations with flexible superstructure and varying degrees of abutment restraint [121]. The responses were found to be in a very good agreement in the majority of cases with those obtained by the dynamic analysis. The multimode adaptive pushover procedure was adopted and recommended for the seismic performance evaluation of integral bridges in another study [120].

Demand Spectrum

Demand curve is represented by earthquake response spectra represented at various levels of damping. Acceleration response spectra represent the graphical variation of spectral acceleration, (S_{ae}) with natural period (T_n) coordinates. In order to illustrate the relationship between S_{ae}, and spectral displacements S_{de}

for the demand, the standard elastic acceleration response spectrum is converted to ADRS format (*Fig. 5(c)*) by replacing T_n with the S_{de} coordinates in the abscissa corresponding to the S_{de} ordinates employing Eq.(31) as,

$$S_{de} = S_{ae}(\frac{T_n}{2\pi})^2 \quad (31)$$

The obtained elastic demand spectrum is further converted to inelastic demand spectrum in order to account for the inelastic structural behaviour. The relationship between damped linear elastic response spectra and the inelastic response spectra are presented such that elastic damping ratios can be related to ductility ratios for various characteristics of hysteresis behavior. The damping that occurs when an earthquake ground motion drives a structure into the inelastic range can be viewed as a combination of the inherent viscous damping in a structure and hysteresis damping. Many researchers have adopted different spectral reduction factors.

In one study, the relationships were developed where the elastic response was reduced by $1/\sqrt{2\mu - 1}$ in the constant acceleration portion of the response spectrum and by $1/\mu$ in the constant velocity portion [129]. For an inelastic SDOF system with bilinear force-deformation characteristics, the relationship between the elastic spectra for a viscous damping ratio and the inelastic spectra, defined by S_{ae} and S_{de} co-ordinates, was developed [130] as,

$$S_a = \frac{S_{ae}}{R_\mu}, \quad S_d = \frac{\mu}{R_\mu} S_{de} = \frac{\mu}{R_\mu}\frac{T_n^2}{4\pi^2} S_{ae} = \mu\frac{T_n^2}{4\pi^2} S_a \quad (32)$$

where μ is ductility factor defined as the ratio between the maximum displacement and the yield displacement, and R_μ is the reduction factor, which represents the hysteresis energy dissipation of ductile structures for a specified ductility ratio as given below,

$$R_\mu = (\mu - 1)\frac{T_n}{T_c} + 1; \qquad T_n < T_c \quad (32)$$

$$R_\mu = \mu; \qquad T_n > T_c \quad (34)$$

where T_c is the characteristic period of the ground motion, typically defined as the transition period at the junction of constant acceleration segment (short period range) and the constant velocity segment of the spectrum (medium period range).

Another study calculated the equivalent viscous damping for the whole system (pier-deck assemblages) for each chosen performance level (PL) based on the Jacobsen's equations for bearings and piers [48] as,

$$\xi_{b,j} = \frac{E_{visc}+E_{hyst}+E_{fr}}{2\pi\cdot F_{PL}\cdot d_{PL}}, \; \xi_{p,j} = \xi_0 + \xi_{eq} = 0.05 + \frac{1}{\pi}(1 - \frac{(1-r)}{\sqrt{\mu}} - r\mu) \quad (35)$$

where: d_{PL} is the displacement of the device at the PL,
F_{PL} is the corresponding force level,
E_{visc}, E_{hyst} and E_{fr} are the energy loss in the bearing device, through

viscous, hysteretic or frictional behaviour, in a cycle of amplitude d_{PL} ,

$\xi_{b,j}$ is the equivalent damping of the jth bearing device

ξ_0 is the viscous damping of pier

ξ_{eq} is the equivalent hysteretic damping of the pier,

$\xi_{p,j}$ is the equivalent damping of jth pier

μ is its displacement ductility,

r is the strain hardening ratio of the pier force-displacement curve.

The equivalent damping values of each of the pier-bearings system is then computed, by combining the damping values of pier and bearing devices in proportion to their individual displacements, $d_{p,j}$ and $d_{b,j}$ respectively as,

$$\xi_j = \frac{\xi_{b,j} d_{b,j} + \xi_{p,j} d_{p,j}}{d_{b,j} + d_{b,j}} \tag{36}$$

Finally the equivalent damping, ξ_{PL} for the whole bridge system is obtained by weighing the damping values of each jth bearing-pier system, (Eq.(36)) in proportion to the corresponding force levels, F_j with respect to the total base shear, V_b from Eq. (37) as,

$$\xi_{PL} = \frac{\sum_{j=1}^{n} \xi_j \cdot F_j}{\sum_{j=1}^{n} F_j} = \frac{\sum_{j=1}^{n} \xi_j \cdot F_j}{V_b} \tag{37}$$

A proper reduction factor, η is to be calculated based on $\xi_{total,PL}$ using which the damped elastic demand spectrum is to be reduced as calculated from Eq. (38) [131] or similar such equation,

$$\eta = \sqrt{\frac{7}{2 + \xi_{total,PL}}} \quad \text{with limitation } \eta > 0.55 \tag{38}$$

Performance Point

When the capacity and demand curves are superimposed on each other, the relationship between the demand and capacity is readily apparent. If the capacity curve can break through the demand envelope, the structure can survive the earthquake. The graphical intersection of the two curves determines the performance levels of the structure for that earthquake. Using the most recent improvement in pushover technique, i.e., the adaptive pushover analysis, Adaptive Capacity Spectrum was introduced [121] wherein the capacity spectrum of the bridge is derived step-by step within an adaptive perspective from the equivalent system displacement $S_{d,k}$. This is combined with the elements from the direct displacement based design method [132], and acceleration $S_{a,k}$, based on the actual deformed shape of the bridge at each

analysis step, k (Eqs.(39-41)). The developed adaptive capacity spectrum is intersected with the demand spectrum, providing an estimate of the inelastic acceleration and displacement demand (i.e., performance point) on the structure as shown in *Fig. 6*.

$$S_{d,k} = \frac{\sum_j m^*_{j.k} D^2_{j.k}}{\sum_j m^*_{j.k} D_{j,k}} \tag{39}$$

$$S_{a,k} = \frac{V_{b,k}}{M_{e,k} g} \tag{40}$$

$$M_{e,k} = \frac{\sum_j m^*_{j.k} D_{j,k}}{S_{d,k}} \tag{41}$$

where: $V_{b,k}$ is the base shear of the bridge
$m^*_{j.k}$ is the participating mass of the jth pier-bearings assemblage
$D_{j,k}$ is the horizontal displacement of the jth pier-bearings system at the analysis step, k
$M_{e,k}$ is the effective mass of the bridge as a whole

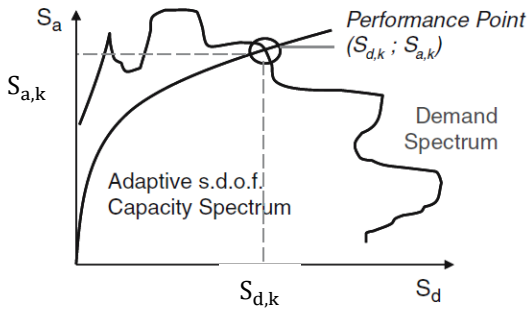

Figure 6. Location of the performance point from the demand and the capacity spectra [121]

Development of Fragility Curve

Using CSM, fragility curve can be generated by two ways:

i) The first method is to find the performance point (i.e., the damage state) of the structure under a predefined seismic intensity (i.e., a given PGA) using an overdamped demand spectrum derived by an iterative procedure for an idealized bilinear capacity curve [133]. To account for uncertainties in earthquake parameters (as discussed in sections 2.3 and 2.4), mean and mean ± standard deviation demand response spectra can be generated considering a suite of ground motion histories sorted by PGA specific to the purpose. Similarly bridge samples can be generated considering structural uncertainties. Then a capacity spectrum for each sample bridge is constructed successively and merged with a mean and mean ± standard deviation demand spectra for a particular PGA group [66]. Hence three performance points with three corresponding spectral

displacements $\overline{S_d}(a)$ and $\overline{S_d}(a) \pm \sigma_d(a)$ are defined for each bridge sample for a PGA value a. The two parameters, median and standard deviation of the lognormal distribution for the spectral displacement $S_d(a)$ can be obtained from the following equation as,

$$\overline{S_d}(a) = c(a)\exp\left[\{\xi(a)\}^2/2\right], \{\sigma_d(a)\}^2 = \{\overline{S_d}(a)\}^2[\,(\{\xi(a)\}^2) - 1] \quad (42)$$

Thereafter, the probability that the sample bridge j will have a state of damage exceeding the limit displacement d_l is given by,

$$P[S_d(a) \geq d_l \text{ for sample bridge j}] = P_j(a, d_l) = 1 - \Phi\left[\frac{\ln\left(\frac{d_{l,j}}{c_j}\right)}{\xi_j(a)}\right] \quad (43)$$

The fragility for that value of PGA for the damage state corresponding to d_l can be estimated by taking all K number of bridges in the PGA group under consideration as below,

$$F(a, d_l) = \frac{\sum_{j=1}^{K} P_j(a,d_l)}{K} \quad (44)$$

ii) The second method is to evaluate the seismic intensity (i.e., the PGA) of the expected ground motions, corresponding to pre-determined damage states of the structure, identified by given performance points on the capacity curve of the bridge. The inelastic deformed shape of the bridge corresponding to each damage state, therefore, is already known at the beginning of the analysis. As a consequence, the equivalent damping ratio of the bridge can be directly evaluated by properly combining the damping contributions of the single bridge components [133]. Compared to the first method, this method is not iterative and does not require the linearization of the capacity curve of the equivalent SDOF system of the bridge.

The PGA value associated with each adopted performance level, PL, is evaluated graphically by translating the normalized demand spectrum to intercept the capacity spectrum at that PL (*Fig. 7(a)*). It can be calculated analytically as the ratio between the acceleration value on the capacity curve, $S_{a,PL}$ corresponding to each PL and the spectral acceleration $S_{a1,PL}$ at the effective period of acceleration T_{PL} of the demand spectrum (which is reduced for the effective viscous damping ξ_{PL} (Eq.(37)) using Eq.(45) as,

$$PGA_{PL} = \frac{S_{a,PL}}{S_{a1}(T_{PL},\xi_{PL})}, \quad T_{PL} = 2\pi\sqrt{\frac{M_{PL}}{K_{PL}}} = 2\pi\sqrt{\frac{S_{d,PL}}{g \cdot S_{a,PL}}} \quad (45)$$

The evaluated PGA value associated with each PL represents the median threshold value of PGA of the associated ground motion. Starting from these values, a series of fragility curves are developed, one for each PL. The fragility curve which represents the probability of exceedance of a PL, as a function of PGA of the expected ground motion is expressed by a lognormal cumulative probability function, as in Eq.(46) and the evaluated curve for a particular PL is

shown in *Fig. 7(b).*

$$P(DS \geq PL|PGA) = \Phi\left[\frac{1}{\beta_c}\ln\left(\frac{PGA}{PGA_{PL}}\right)\right] \quad (46)$$

where LHS of the equation represents the probability of the Damage State (DS) being equal to or exceeding the selected Performance Level (PL) for a given seismic intensity (for e.g., PGA), Φ is the standard normal cumulative probability function, PGA_{PL} the median threshold value of PGA associated with the selected PL and β_c the total lognormal standard deviation which takes into account the uncertainties related to the input ground motion, bridge response, etc.

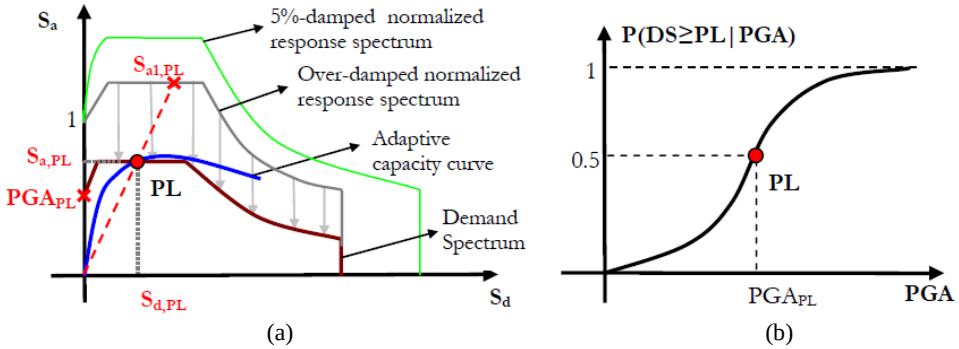

Figure 7. (a) Evaluation of PGA for each PL [48] (b) The corresponding fragility curve for each PL [48]

3. CRITIQUE

Though significant research work in the field of vulnerability assessment has been carried out and is still going on for most of the bridge typologies in various regions worldwide, the modeling methodologies require refinements in various aspects in order to obtain a more realistic and hence reliable vulnerability estimates.

Most of the studies adopted simplified foundation-soil system considering it either to be fixed or modeled as springs, with emphasis on structural details, whereas some studies focussed mainly on soil-foundation interaction elements along with simplified structural components [29]. Only a few studies worked on detailed bridge-soil-foundation system (BSFS) elements [6, 7, 38, 88, 89, 90]. Also since most of the researchers did not model the foundation, damage limit states related to pile behaviour are very few. Limit states for foundation were based on both pile design and the soil profiles in which piles were embedded, i.e., with lateral pile-ground interactions. However, the identified damage states are based on only pile structural damages and failures. The failure criteria of soil also need to be considered while identifying damages to the soil-pile system. Deficiencies exist in the bridge structural modeling technique in most

of the studies for not modeling bar-slip effect at the cap beam-column and column-foundation connections. Various joint models, i.e., joint failures as well as cap beam damages are not included in most studies. Hence, these issues also need to be addressed for better and more realistic vulnerability estimates of bridges. To characterize the ground motion, most researchers have adopted PGA and spectral parameters at the fundamental period as the ground motion intensity measure (IM) when assessing the fragility of bridges. PGA is not an ideal IM for many cases. For systems prone to cumulative damage, such as degrading and geotechnical systems, better IMs (like Arias intensity) should account for duration (number of significant cycles) and the energy content of the record. For example, spectral acceleration at the fundamental period is not found to be an optimal choice for intensity measure for integral abutment bridges. The current IMs are found to capture poorly the effects of classes of ground motions like near-fault ground motions containing velocity pulse. While investigating for optimal IM and to improve the dispersions of PSDMs, optimal vector-valued IMs, displaying a good correlation with the adopted EDPs are required to be identified.

4 CONCLUSIONS

This paper discusses the key ingredients involved in generating the analytical fragility curves for bridges and the step by step methodology for the curve development. Following the devastating consequences of the previous earthquakes, researches promptly headed in the direction of seismic vulnerability evaluation of existing bridge/bridge classes in the respective regions or of a particular structural configuration with certain earthquake scenario, which is a part and parcel of seismic risk mitigation. The basis of the assessment methodologies adopted worldwide is the same and has been summarised in a generalized way.

Identification of structure type (on the basis of different parameters relevant to their seismic performance) is emphasized as an essential step towards generating the suitable fragility function for the risk study. Different structural configurations (e.g., column detailing, superstructure type, material, connection, continuity at support and foundation type, etc.) lead to differences in damage resistant capabilities for bridges [95], hence signifying their inherent impact on the resulting fragility functions. The damage functions for a structural type are specific and should be evaluated from the damage patterns observed or determined on the basis of analysis of appropriate structural models demonstrating the realistic behavior of the bridge type. Foundation-soil interaction effect becomes increasingly important with the increase in intensity of the ground shaking [134]. Hence SSI effects should be precisely modeled along with monitoring of pile structural damage and damage pattern of surrounding soil. Damage states should be defined and limits should be

evaluated based on the damage sequence observed. While evaluating the bridge fragility through NLTHA and for the generation of a precise PSDM, the relation between ground motion IMs and structural demand should be well explored to decrease the variability in PSDMs. Some errors or bias are introduced into the PSDA method due to a single assumption relating EDP to IM despite the damage states. The power-law form of the demand model is often a good structural response predictor for nonlinear response; however, it does not necessarily accurately capture the structural response over the complete range of intensities considered. Errors arise when considering highly nonlinear behaviour, global instability or collapse. In these instances, the probability mass of, for example, collapse needs to be accounted for explicitly. Therefore, the power-law form of the demand model should be understood as a local approximation [69]. The lack of large intensity earthquake motion records may introduce some error in the PSDA results as the input motions are biased toward smaller intensity [95]. Hence the IDA forms a better and more reliable option for generating PSDMs because the fragility functions are based on many more simulation cases. Also no pre-adopted relationship between the EDP and IM is required to be assumed inspite of some possible bias from the record scaling process. Further, defining a proper IM is essential to reduce the uncertainties associated with PSDMs while catering for more accurate fragility estimates [10]. However, determining the optimum IM is still a challenge especially for BSFS with significant variability in soil and structural characteristics. Vector-valued intensity measures can be used to eliminate bias and increase the efficiency of structural response prediction [94]. Due to the inherent complexities of NLTHA, many researchers opt for CSM for generating fragility curves. As compared to all the variants of pushover analysis, the DAP has led to significant improvement in the agreement between static and dynamic analysis results due to consideration of spectrum scaling, higher mode contributions, alteration of local resistance and modal characteristics induced by the accumulated damage, accurate estimation of deformation profile and capacity curves. The innovative DAP not only constitutes an extremely appealing tool to obtain the response information close to that predicted by NLTHA, but also the entire structural assessment exercise becomes coherent with direct use of displacements in the recent seismic assessment trends.

REFERENCES

[1] Priestley, MJN, Seible, F, Calvi, GM, *Seismic Design and Retrofit of Bridges*, John Wiley & Sons, New York, 1996.

[2] AmiriHormozaki, E, Pekcan, G, Itani, A, "Analytical fragility functions for horizontally curved steel I- girder highway bridges" , Earthquake Spectra, 2014.

[3] Tecchio, G, Grendene, M, Modena, C, 'Spatial variability of earthquake ground motion: effects on seismic response of long multi-span girder bridges", *Proc. 8th Intl. Conference on Structural Dynamics, EURODYN*, Leuven, Belgium, 4-6 July 2011.

[4] Kim, SH, Feng, MQ, "Fragility analysis of bridges under ground motion with spatial

variation", International Journal of Non-Linear Mechanics, Vol. 38, pp. 705 – 721, 2003.
[5] Avsar, O, "Fragility Based Seismic Vulnerability Assessment of Ordinary Highway Bridges in Turkey", Ph.D. Thesis, The Graduate School of Natural and Applied Sciences of Middle East Technical University, 2009.
[6] Wang, Z, Padgett, JE, Dueñas-Osorio, L, "Influence of Vertical Ground Motions on the Seismic Fragility Modeling of a Bridge-Soil-Foundation System", Earthquake Spectra, Vol. 29, No. 3, pp. 937–962, 2013.
[7] Aygün, B, Dueñas-Osorio, L, Padgett, JE, DesRoches, R, "Efficient Longitudinal Seismic Fragility Assessment of a Multispan Continuous Steel Bridge on Liquefiable Soils", Journal of Bridge Engineering, Vol. 16, pp. 93-107, 2011.
[8] Serdar, N, Jankovic, S, "Performance –based seismic assessment of continuous concrete bridge with lack of confining reinforcement", *Proc.* 2nd *European Conference on Earthquake Engineering and Seismology*, Istanbul, 2014
[9] Karim, KR, Yamazaki, F, "Effect of earthquake ground motions on fragility curves of highway bridge piers based on numerical simulation", Earthquake Engineering and Structural Dynamics, Vol. 30, pp. 1839–1856, 2001.
[10] Zelaschi, C, Monteiro, R, Marques, M, Pinho, R, "Comparative Analysis of Intensity Measures for Reinforced Concrete Bridges. *Proc.* 2nd *European Conference on Earthquake Engineering and Seismology*, Istanbul, 2014
[11] Mackie, K, Stojadinovic, B, "Fragility Curves for Reinforced Concrete Highway Overpass Bridges", *Proc. 13th World Conference on Earthquake Engineering*, Vancouver, B.C., Paper No. 1553, Canada, 2004(a).
[12] Choi, E, DesRoches, R, Neilson, B, "Seismic fragility of typical bridges in moderate seismic zones", Engineering Structures, Vol. 26, pp. 187–199, 2004.
[13] DesRoches, R, Choi, E, Leon, RT, Dyke, SJ, Aschheim, M, "Seismic Response of Multiple Span Steel Bridges in Central and Southeastern United States. I: As Built", Journal of Bridge Engineering, Vol. 9, pp. 464-472, 2004.
[14] Ramanathan, K, DesRoches, R, Padgett, JE, "Analytical Fragility Curves for Multispan Continuous Steel Girder Bridges in Moderate Seismic Zones", Journal of the Transportation Research Board, No. 2202, Transportation Research Board of the National Academies, Washington, pp. 173–182, 2010.
[15] Ramanathan, K, Padgett, JE, DesRoches, R, "Fragility Curves for Typical Multispan Simply Supported Bridge Classes in Moderate Seismic Zones: Pre- and Post-Seismic Design Considerations*", Proc. 3rd ECCOMAS Thematic Conference on Computational Methods in Structural Dynamics and Earthquake Engineering, COMPDYN*, M. Papadrakakis, M. Fragiadakis, V. Plevris (eds.) Corfu, Greece, 25–28 May 2011.
[16] Nielson, BG, DesRoches, R, "Analytical Seismic Fragility Curves for Typical Bridges in the Central and Southeastern United States*",* Earthquake Spectra, Vol. 23, No. 3, pp. 615–633, 2007(a).
[17] Nielson BG and DesRoches R. Seismic Performance Assessment of Simply Supported and Continuous Multispan Concrete Girder Highway Bridges. *Journal of Bridge Engineering* Vol. 12, No. 5, pp. 611-620, 2007(b).
[18] Sullivan, IT, "Analytical Seismic Fragility Curves for Skewed Multi-Span Steel Girder Bridges", MSc. Thesis, Civil Engineering, the Graduate School of Clemson University, 2010.
[19] Dicleli, M, Bruneau, M, "Seismic Performance of Multipan Simply Supported Slab-on Girder Steel Highway Bridges", Journal of Structural Engineering, Vol. 121, pp. 1497-1506, 1995(a)
[20] Dicleli, M, Bruneau, M, "Seismic Performance of Single-Span Simply Supported and Continuous Slab-on- Girder Steel Highway Bridges", Journal of Structural Engineering Vol. 121, pp. 1497-1506, 1995(b)
[21] Dicleli, M, Bruneau, M, "Quantative Approach to Rapid Seismic Evaluation of Slab-on-Girder Steel Highway Bridges", Journal of Structural Engineering, Vol. 122, pp. 1160-1168,

1996.
[22] Shinozuka, M, Feng, MQ, Kim, HK, Kim, SH, "Nonlinear Static Procedure for Fragility Curve Development", Journal of Engineering Mechanics, Vol. 126, pp. 1287-1295, 2000(a).
[23] Shinozuka, M, Feng, MQ, Lee, J, Naganuma, T, "Statistical Analysis of Fragility Curves", Journal of Engineering Mechanics, Vol. 126, pp. 1224-1231, 2000(b).
[24] Jernigan, JB, Hwang, H, "Development of bridge fragility curves", Proc. *7th US National Conference on Earthquake Engineering*, 2002.
[25] Hwang, H, Liu, JB, Chiu, Y, "Seismic Fragility Analysis of Highway Bridges", Technical Report, MAEC RR-4 Project, July 2001.
[26] Zhong, J, Gardoni, P, Rosowsky, D, Haukaas, T, "Probabilistic Seismic Demand Models and Fragility Estimates for Reinforced Concrete Bridges with Two-Column Bents", Journal of Engineering Mechanics, Vol. 134, pp. 495-504, 2008.
[27] Abdel-Mohti, A, Pekcan, G, "Assessment of seismic performance of skew reinforced concrete box girder bridges", International Journal of Advanced Structural Engineering, Vol. 5, No. 1, pp.1-18, 2013.
[28] Zhang, J, Huo, Y, Brandenberg, SJ, Kashighandi, P, "Effects of structural characterizations on fragility functions of bridges subject to seismic shaking and lateral spreading", Earthquake Engineering & Engineering Vibration, Vol. 7, pp. 369-382, 2008.
[29] Brandenberg, SJ, Kashighandi, P, Zhang, J, Huo, Y, Zhao, M, 'Fragility Functions for Bridges in Liquefaction-Induced Lateral Spreads", Earthquake Spectra, Vol. 27, No. 3, pp. 683– 717, 2011.
[30] Zakeri, B, Padgett, JE, Amiri, GG, "Fragility Analysis of Skewed Single-Frame Concrete Box-Girder Bridges", Journal of Performance of Constructed Facilities, Vol. 28, pp. 571-582, 2014.
[31] Kunnath, SK, Larson, L, Miranda, E, "Modelling considerations in probabilistic performance- based seismic evaluation: case study of the I-880 viaduct. Earthquake Engineering and Structural Dynamics, Vol. 35, pp. 57–75, 2006.
[32] Meng, JY, Lui, EM, "Seismic analysis and assessment of a skew highway bridge", Engineering Structures, Vol. 22, pp. 1433–1452, 2000.
[33] Jeon, JS, Shafieezadeh, A, Lee, DH, Choi, E, DesRoches, R, "Damage assessment of older highway bridges subjected to three-dimensional ground motions: characterization of shear–axial force interaction on seismic fragilities", Engineering Structures, Vol. 87, pp. 47-57, 2015.
[34] Pan, Y, Agrawal, AK, Ghosn, M, "Seismic Fragility of Continuous Steel Highway Bridges in New York State", Journal of Bridge Engineering, Vol. 12, pp. 689-699, 2007.
[35] Pan, Y, Agarwal, AK, Ghosn, M, Alampalli, S, "Seismic Fragility of Multispan Simply Supported Steel Highway Bridges in New York State. II: Fragility Analysis, Fragility Curves, and Fragility Surfaces", Journal of Bridge Engineering, Vol. 15, pp. 462-472, 2010(a).
[36] Seo, J, Linzell, DG, "Horizontally curved steel bridge seismic vulnerability assessment", Engineering Structures, Vol. 34, pp. 21–32, 2012.
[37] Saadeghvaziri, MA, Yazdani-Motlagh, AR, "Seismic behavior and capacity/demand analyses of three multi-span simply supported bridges", Engineering Structures, Vol. 30, pp. 54–66, 2007.
[38] Kwon, OS, Elnashai, AS, "Fragility analysis of a highway over-crossing bridge with consideration of soil–structure interactions", Structure and Infrastructure Engineering, Vol. 6, No. 1-2, pp. 159–178, 2010.
[39] Bignell, JL, LaFave, JM, Hawkins, NM, "Seismic vulnerability assessment of wall piers supported highway bridges using nonlinear pushover analyses", Engineering Structures, Vol. 27, pp. 2044–2063, 2005.
[40] Tavares, DH, Padgett, JE, Paultre, P, "Fragility curves of typical as-built highway bridges in eastern Canada", Engineering Structures, Vol. 40, pp. 107–118, 2012.

[41] Tavares, DH, Suescun, JR, Paultre, P, Padgett, JE, "Seismic Fragility of a Highway Bridge in Quebec", Journal of Bridge Engineering, Vol. 18, pp. 1131-1139, 2013.
[42] Siddiquee, KN, "Seismic vulnerability assessment of wall pier highway bridges in British Columbia", Master of Applied Science Thesis, University of British Columbia, 2015.
[43] Colina, JD, Eberhard, MO, Ryter, SW, Wood, SL, "Sensivity of Seismic Assessment of a Double-Deck, Reinforced Concrete Bridge", Earthquake Spectra, Vol. 12, No. 2, 1996.
[44] Ballard, TA, Sedarat, H, "SR5 Lake Washington Ship Canal Bridge pushover analysis", Computers and Structures, Vol. 72, pp. 63-80, 1999.
[45] Mwafy, AM, Kwon, OS, Elnashai, A, Hashash, YM, "Wave passage and ground motion incoherency effects on seismic response of an extended bridge", Journal of Bridge Engineering, Vol. 16, No. 3, pp. 364-374, 2010.
[46] Gòmez-Soberón, MC, Soria-Rodríguez, I, "Vulnerability Evaluation of Common Simple-Suppported Bridges", 2014.
[47] Torbol, M, Shinozuka, M, "The directionality effect in the seismic risk assessment of highway networks", Structure and Infrastructure Engineering, Vol. 10, No. 2, pp. 175-188, 2014.
[48] Cardone, D, Perrone, G, Dolce, M, "Seismic risk assessment of highway bridges, *Proc. 1st US–Italy Seismic Bridge Worksho*p, IUSS Press Ltd, Pavia (Italy), 2007.
[49] Franchetti, P, Grendene, M, Sleiko, D, Modena, C, "Seismic damage assessment for six RC bridges in the Veneto region (NE Italy), Bollettino di geofisica applicate, Vol. 49, No. 3-4, pp. 513-532, 2008.
[50] Moschonas, IF, Kappos, AJ, Panetsos, P, Papadopoulos, V, Makarios, T, Thanopoulos, P, "Seismic fragility curves for Greek bridges: methodology and case studies", Bull Earthquake Engineering, Vol. 7, pp. 439–468, 2009.
[51] Pottatheere, P, Renault, P, "Seismic Vulnerability Assessment of Skew Bridges", *Proc. 14th World Conference on Earthquake Engineering*, Beijing, China, October 12-17, 2008.
[52] Zsarnoczay, A, Vigh, LG, Kollar, LP, "Seismic Performance of Conventional Girder Bridges in Moderate Seismic Regions", Journal of Bridge Engineering, Vol.19, No. 1-9, 2014.
[53] Simon, J, "Seismic performance and damage assessment of hungarian road bridges", 2016.
[54] Bradley, BA, Cubrinovski, M, Dhakal, RP, MacRae, GA, "Probabilistic seismic performance and loss assessment of a bridge–foundation–soil system", Soil Dynamics and Earthquake Engineering, Vol. 30, No. 5, pp. 395-411, 2010.
[55] Nicknam, A, Mosleh, A, Jamnani, HH, "Seismic Performance Evaluation of Urban Bridge using Static Nonlinear Procedure, Case Study: Hafez Bridge", Procedia Engineering, Vol. 14, pp. 2350–2357, 2011.
[56] Nateghi, F, Shahsavar, VL, "Development of fragility and reliability curves for seismic evaluation of a major prestressed concrete bridge", *Proc. 13th World Conference On Earthquake Engineering*, Vancouver, August 2004.
[57] Kibboua, A, Bechtoula, H, Mehani, Y, Naili, M, "Vulnerability assessment of reinforced concrete bridge structures in Algiers using scenario earthquakes", Bull Earthquake Engineering, Vol. 12, pp. 807–827, 2014.
[58] Parool, N, Rai, DC, "Seismic Fragility of Multi-Span Simply Supported Bridge with Drop Spans and Steel Bearings", Proc. 10th U.S. *National Conference on Earthquake Engineering Frontiers of Earthquake Engineering*, Anchorage, Alaska, July 21-25, 2014.
[59] Tomar, R, Nimoriya, MK, Singh, S, "Seismic Vulnerability Assessment of Bridges using Fragility - Based Approach", Global Journal of Engineering Science and Research Management, 2016.
[60] Chang, DW, Cheng, MY, Chang, TL, "Seismic Assessment and Retrofit Strategy of Taiwan Roadway Bridges", *Proc. 14th World Conference on Earthquake Engineering*, Beijing, China, October 12-17, 2008.
[61] Liao, WI, Loh, CH, "Preliminary Study on the Fragility Curves for Highway Bridges in

Taiwan", Journal of the Chinese Institute of Engineers, Vol. 27, No. 3, pp. 367-375, 2004.
[62] Sung, YC, Hsu, CC, Hung, HH, Chang, YJ, "Seismic risk assessment system of existing bridges in Taiwan", Structure and Infrastructure Engineering, Vol. 9, No. 9, pp. 903-917, 2013.
[63] Lee, SM, Kim, TJ, Kang, SL, 'Development of fragility curves for bridges in Korea", KSCE Journal of Civil Engineering, Vol. 11, No. 3, pp. 165-174, 2007.
[64] Tanaka, S, Kameda, H, Nojima, Ohnishi, S, "Evaluation of seismic fragility for highway transportation systems", *Proc. 12th World Conference on Earthquake Engineering*, Paper No. 0546, Upper Hutt, New Zealand, January, 2000.
[65] Elnashai, AS, Borzi, B, Vlachos, S, "Deformation-based Vulnerability functions for RC bridges", Structural Engineering and Mechanics, Vol. 17, No. 2, pp. 215-244, 2004.
[66] Shinozuka, M, Feng, MQ, Kim, HK, Uzawa, T, Ueda, T, "Statistical Analysis of Fragility Curves", Technical Report MCEER, Department of Civil and Environment Engineering, University of Southern California, Federal Highway Administration, Contract No. DTFH61 92-C-00106, 2001.
[67] Neilson, BG, "Analytical Fragility Curves for Highway Bridges in Moderate Seismic Zones", Ph.D. Thesis, School of Civil and Environmental Engineering, Georgia Institute of Technology, 2005.
[68] Zhang, J, Huo, Y, "Evaluating effectiveness and optimum design of isolation devices for highway bridges using fragility function method", Engineering Structures, Vol. 31, No. 8, pp. 1648–1660, 2009.
[69] Mackie, K, Stojadinović, B, "Performance-Based Seismic Bridge Design for Damage and Loss Limit States", Earthquake Engineering and Structural Dynamics, Vol. 36, No. 13, pp. 1953–1971, 2007.
[70] Nielson, BG, DesRoches, R, "Seismic fragility methodology for highway bridges using a component level approach", Earthquake Engineering and Structural Dynamics, Vol. 36, No. 6, pp. 823-839. DOI:10.1002/eqe.655, 2007(b).
[71] Ramanathan, K, DesRoches, R, Padgett, JE, "A comparison of pre- and post-seismic design considerations in moderate seismic zones through the fragility assessment of multispan bridge classes. Engineering Structures, Vol. 45, pp. 559–573, 2012.
[72] HAZUS: Earthquake loss estimation methodology, Technical Manual, 1997.
[73] Berry, M, Eberhard, MO, "Performance models for flexural damage in reinforced concrete columns", 2003.
[74] Hose, Y, Silva, P, Seible, F, "Development of a Performance Evaluation Database for Concrete Bridge Components and Systems under Simulated Seismic Loads", Earthquake Spectra, Vol. 16, No. 2, pp. 413–442, 2000.
[75] SEAOC: Seismic design manual, Structural engineering association of California, 2000.
[76] Mehanny, SSF, Ramadan, OMO, Howary, HAE, "Assessment of bridge vulnerability due to seismic excitations considering wave passage effects", Engineering Structures, Vol. 70, pp. 197–207, 2014.
[77] Dutta, A, Mander, JB, "Rapid and detailed seismic fragility analysis of highway bridges", Unpublished Technical Report MCEER, 2001.
[78] FHWA: Federal Highway Administration, Seismic retrofitting manual for highway bridges, Publication No. FHWA-RD-94-052, Office of Engineering and Highway Operations R&D, McLean, 1995.
[79] Yi, JH, Kim, SH, Kushiyama, S, "PDF interpolation technique for seismic fragility analysis of bridges", Engineering Structure, Vol. 29, pp. 1312-22, 2007.
[80] Akbari, R, "Seismic fragility analysis of reinforced concrete continuous span bridges with irregular configuration", Structure and Infrastructure Engineering, Vol. 8, No. 9, pp. 873-889, 2012.
[81] Basu, BS, Shinozuka, M, "Effect of ground motion directionality on fragility characteristics of a highway bridge", Advances in Civil Engineering, 2011.

[82] Mounnarath, P, Schmitz, U, Zhang, Ch, "Seismic fragility assessment of continuous integral bridge frames with variable expansion joint clearances", World Academy of Science, Engineering and Technology, International Journal of Civil, Environmental, Structural, Construction and Architectural Engineering, Vol 10, No. 2, 2016.
[83] Kowalsky, MJ, "Deformation Limit States for Circular Reinforced Concrete Bridge
Columns", ASCE Journal of Structural Engineering, Vol. 126, No. 8, pp. 869-878, 2000.
[84] Mander, JB, Kim, DK, Chen, SS, Premus, GJ, "Response of Steel Bridge Bearings to Reversed Cyclic Loading", Techical Report, NCEER-96-0014, November 13, 1996
[85] Naeim, F, Kelly, JM, *Design of seismic isolated structures: From theory to practice*, John Wiley & Sons, New York, 1999
[86] Wang, J, "Piers and Columns", Bridge Engineering Handbook, W.-F. Chen and L. Duan, eds., CRC Press, 2000.
[87] Caltrans: California Department of Transportation, "Bridge design aids", Sacramento, CA, 1st Edition, 1999.
[88] Bradley, BA, Cubrinovski, M, Dhakal, RP, MacRae, GA, "Intensity measures for the seismic
response of pile foundations", Earthquake Engineering and Soil Dynamics, Vol. 29, No. 6, pp. 1046–1058, 2009.
[89] Ledezma, C, "Performance-based earthquake engineering design evaluation procedure for bridge foundations undergoing liquefaction induced lateral spreading" Ph.D. dissertation, University of California, Berkeley, 2007.
[90] Padgett, JE, Ghosh, J, Dueñas-Osorio, L, "Effects of liquefiable soil and bridge modeling parameters on the seismic reliability of critical structural components", Structure and Infrastructure Engineering, Vo. 9, No. 1, pp. 59-77, 2013.
[91] Song, ST, Chai, YH, Hale, TH, "Analytical model for ductility assessment of fixed-head concrete piles", Journal of Structural Engineering, Vol. 131, No. 7**,** pp. 1051–1059, 2005.
[92] Basu, D, Prezzi, M, "Analysis of Laterally Loaded Piles in Multilayered Soil Deposits", Final Report FHWA/IN/JTRP, Project No. C-36-36LL, File No. 6-14-38 SPR-2630, 2007.
[93] Masahiro, S, Kohno, T, Nakatani, S, "Geotechnical criteria for serviceability limit state of horizontally loaded deep foundations", *Proc. 2nd Intl. Symposium on Geotechnical Risk and Safety*, 2009:119-126, 2009.
[94] Baker, JW, Cornell, CA, "Vector-Valued Ground Motion Intensity Measures for Probabilistic Seismic Demand Analysis", PEER Report 2006/08. Pacific Earthquake Engineering Research Center College of Engineering University of California, Berkeley, 2006.
[95] Zhang, J, Huo, Y, Brandenberg, SJ, Kashighandi, P, "Effects of structural characterizations on fragility functions of bridges subject to seismic shaking and lateral spreading", Earthquake Engineering & Engineering Vibration, Vo. 7, pp. 369-382, 2008.
[96] Mackie, K, Stojadinović, B, "Seismic Demands for Performance-based Design of Bridges", PEER Report No.16, Pacific Earthquake Engineering Research Center, University of California, Bekerley, CA, 2003.
[97] Padgett, JE, Nielson, BG, DesRoches, R, "Selection of optimal intensity measures in probabilistic seismic demand models of highway bridge portfolios", Earthquake Engineering and Structural Dynamics, Vol. 37, pp. 711–725, 2008.
[98] Taskari, O, Sextos, A, "Multi-angle, multi-damage fragility curves for seismic assessment of bridges", Earthquake Engineering & Structural Dynamics, DOI: 10.1002/eqe.2584, 2015.
[99] Padgett, JE, DesRoches, R, "Sensitivity of seismic response and fragility to parameter uncertainty", Journal of Structural Engineering, Vol. 133, No. 12, pp. 1710-1718, 2007.
[100] Pan, Y, Agarwal, AK, Ghosn, M, Alampalli, S, "Seismic Fragility of Multispan Simply

Supported Steel Highway Bridges in New York State. I: Bridge Modeling, Parametric Analysis, and Retrofit Design", Journal of Bridge Engineering, Vol. 15, pp. 448-461, 2010(b)

[101] Monteiro, R, "Sampling based numerical seismic assessment of continuous span RC bridges", Engineering Structures, Vol.118, pp. 407-420, 2016.

[102] Zhang, Y, "Probabilistic structural seismic performance assessment methodology and application to an actual bridge-foundation-ground system", Ph.D. Thesis, University of California, San Diego, 2006.

[103] Mackie, KR, Stojadinovic, B, "Fragility basis for California highway overpass bridge seismic decision making", Report No. 2005/02, Pacific Earthquake Engineering Research Center, University of California, Berkeley, CA, 2005.

[104] Rossetto, T, Elnashai, A, "Derivation of vulnerability functions for European-type RC structures based on observational data", Engineering Structures, Vol. 25, pp. 1241–1263, 2003.

[105] AASHTO: American Association of State Highway and Transportation Officials Standard Specification for Highway Bridges, 16th Edition, Washington, D.C., 1996.

[106] ATC 40: Applied Technology Council, "Seismic Evaluation and Retrofit of Concrete Buildings", Vol. 1, Report No. SSC 96-01, Funded by Seismic Safety Commission, State of California, 1996

[107] Mwafy, A, Elnashai, A, Yen, WH, "Implications of Design Assumptions on Capacity Estimates and Demand Predictions of Multispan Curved Bridges", Journal of Bridge Engineering, Vol. 12, pp. 710-726, 2007.

[108] Choine, MN, O'Connor, AJ, Padgett, JE, "Comparison between the Seismic Performance of Integral and Jointed Concrete Bridges", Journal of Earthquake Engineering, Vol. 19, pp. 172–191, 2015

[109] Mwafy, AM, Kwon, OS, Elnashai, A, Hashash, YMA, "Wave Passage and Ground Motion Incoherency Effects on Seismic Response of an Extended Bridge", Journal of Bridge Engineering, Vol. 16, pp. 364-374, 2011.

[110] Mackie, K, Stojadinovic, B, "Improving Probabilistic Seismic Demand Models through Refined Intensity Measures", *Proc. 13th World Conference on Earthquake Engineering*, Vancouver, B.C., Paper No. 1556, 2004(b).

[111] Ramanathan, K, DesRoches, R, Padgett, JE, "A comparison of pre- and post-seismic design considerations in moderate seismic zones through the fragility assessment of multispan bridge classes", Engineering Structures, Vol. 45, pp. 559–573, 2012.

[112] Saxena, V, Deodatis, G, Shinozuka, M, "Effect of spatial variation of earthquake ground motion on the nonlinear dynamic response of highway bridges", *Proc. 12th World Conference on Earthquake Engineering*, 2000.

[113] Krawinkler, H, Seviratna, GDPK, "Pros and cons of a pushover analysis for seismic performance evaluation", Engineering Structures, Vol. 20, No. 4-6, pp. 452-464, 1998.

[114] Cornell, CA, Krawinkler, H, "Progress and challenges in seismic performance assessment", PEER Center News, Vol.3, No. 2, 2000.

[115] Vamvatsikos, D, Cornell, CA, "Incremental dynamic analysis", Earthquake Engineering and Structural Dynamics, Vol. 31, No. 3, pp. 491-512, 2002.

[116] Rice, JA, *Mathematical statistics and data analysis*, Second Edition, Duxbury Press, Belmont, CA, xx, 602, A49 pp, 1995.

[117] Lehmann, EL, D'Abrera, HJM, *Nonparametrics: Statistical methods based on ranks*, Prentice Hall, Upper Saddle River, N.J., 463 pp, 1998.

[118] Ramanathan, KN, "Next generation seismic fragility curves for California bridges incorporating the evolution in seismic design philosophy" Ph.D. Thesis, Georgia Institute of Technology, 2012.

[119] Freeman, SA, "Development and Use of Capacity Spectrum", Proc. *6th US NCEE Conference on Earthquake Engineering/EERI*, Seattle, Washington, Paper 269, May 31-

June 4, 1998.
[120] Mohtashami, E, Shooshtari, A, "A Multimode Adaptive Pushover Procedure for Seismic Assessment of Integral Bridges", Hindawi Publishing Corporation Advances in Civil Engineering, Article ID 941905, 13 pages, 2013.
[121] Casarotti, C, Pinho, R, "An adaptive capacity spectrum method for assessment of bridges subjected to earthquake action", Bull Earthquake Engineering, Vol. 5, pp. 377–390, 2007.
[122] Chopra, AK, Goel, RK, "Capacity-demand-diagram methods based on inelastic design spectrum", Earthquake spectra, Vol. 15, No. 4, pp. 637-656, 1999.
[123] Chopra, AK, Goel, RK, "A modal pushover analysis procedure for estimating seismic demands for buildings", Earthquake Engineering & Structural Dynamics, Vol. 31, pp. 561–582, 2002.
[124] Paraskeva, TS, Kappos, AJ, "An Improved Multimodal Procedure for Deriving Pushover Curve for Bridges', *Proc. 14th World Conference on Earthquake Engineering*, Beijing, China, October 12-17, 2008,
[125] Lupoi, A, Franchin, P, Pinto, PE, "Further Probing of the Suitability of Push-Over Analysis for the Seismic Assessment of Bridge Structures", *Proc. ECCOMAS Thematic Conference on Computational Methods in Structural Dynamics and Earthquake Engineering (COMPDYN)*, Paper No. 1045, Rethymno, Greece 2007.
[126] Pinho, R, Antoniou, S, Cassarotti, C, Lopez, M, "A Displacement-Based Adaptive Pushover for Assessment of Buildings and Bridges", *NATO International Workshop on Advances in Earthquake Engineering for Urban Risk Reduction*, Istanbul, Turkey, 30th May- 1st June 2005.
[127] Antoniou, S, Pinho, R, "Advantages and Limitations of Adaptive and Non-Adaptive of Force-Based Pushover Procedures", Journal of Earthquake Engineering, Vol. 8, No. 4, pp. 497-522, 2004(a)
[128] Antoniou, S, Pinho, R, "Development and Verification of a Displacement Based Adaptive Pushover Procedure", Journal of Earthquake Engineering, Vol. 8, No. 5, pp. 643-661, 2004 (b).
[129] Newmark, NM, Hall, WJ, "Earthquake spectra and design", Earthquake Research Institute, Oakland, California, 1982.
[130] Vidic, T, Fajfar, P, Fischinger, M, "Consistent inelastic design spectra: strength and displacement", Earthquake Engineering & Structural Dynamics, Vol 23, No. 5, pp. 507-521, 1994.
[131] EN 1998-2, Eurocode 8: Design of structures for earthquake resistance – Part 2: Bridges (2005).
[132] Priestley, MJN, Calvi, GM, "Displacement-Based Seismic Design of Bridges", *1st US–Italy Seismic Bridge Workshop*, 2007
[133] Kappos, AJ, Saiidi, MS, Aydinoglu, MN, Isakovic, T, "*Seismic Design Assessment of Bridges, Inelastic Methods of Analysis and Case Studies*", Geotechnical, Geological and Earthquake Engineering @ Springer, 2012.
[134] Zhang, J, Makris, N, "Seismic Response Analysis of Highway Overcrossings Including Soil-Structure Interaction", PEER Report 2001/02, Pacific Earthquake Engineering Research Center College of Engineering University of California, Berkeley, 2001.